Scuola Internazionale Superiore di Studi Avanzati

Embryonic stem cell-derived neurons form functional networks *in vitro*

Thesis submitted for the degree of Doctor Philosophiae

Neurobiology sector

October 2007

Candidate
Jelena Ban

Supervisor
Vincent Torre

INDEX

1. INTRODUCTION …..……..……1

1.1 STEM CELLS - SOME GENERAL INFORMATION ……..……..1

1.2 DISCOVERY OF ES CELLS ...…….……...2

1.3 PROPERTIES OF ES CELLS ...……...3

1.4 APPLICATION OF STEM CELL TECHNOLOGY……....5

1.4.1 Cell replacement therapy …...……..……..5

1.4.2 Developmental biology …….……6

1.4.3 Drug discovery……...……6

1.5 CULTURE OF ES CELLS ……...……7

1.6 ES CELLS AND NEURONAL DIFFERENTIATION ……9

1.7 PROTOCOLS FOR NEURONAL DIFFERENTIATION OF ES CELLS ……11

1.8 INTRACELLULAR RECORDING OF ES CELLS ……...……..….17

1.9 MEA AND NEURONAL NETWORKS ……...…...……..17

2. MATERIALS AND METHODS…….21

2.1 Reagents and Media ……...……...……..21

2.2 ES-derived neuronal differentiation ……...……...……..21

2.3 Hippocampal culture preparation ……...……..……...23

2.4 Immunocytochemistry ……...…….…...…… 23

2.5 Atomic force microscopy ……...…….24

2.6 Electrophysiological recordings ……...…….……..25

2.7 MEA electrical recordings and electrode stimulation ……...……..26

2.8 Data analysis ……...……27

2.9 Calculation of the mutual information ……...……28

2.10 Calculation of correlation ……...……..29

3. RESULTS……31

3.1 GROWTH AND NEURONAL DIFFERENTIATION OF ES CELLS……..31

3.1.1 Induction of the neuronal differentiation …….33

3.1.2 Amplification of the neuronal precursors ……35

3.1.3 Differentiation of ES-derived precursors ……37

3.2 MATURATION OF ES-DERIVED NEURONS AND CULTURE CHARACTERIZATION ..……37

3.3 INTRACELLULAR RECORDINGS …….48

3.4 ELECTRICAL RECORDINGS ON MEAs ……...…49

3.5 SPONTANEOUS ACTIVITY OF MATURING ES-DERIVED NETWORKS …...53

3.6 SPREAD OF THE EVOKED ELECTRICAL ACTIVITY IN THE NETWORK….59

3.7 REPRODUCIBILITY OF THE RESPONSE AND INFORMATION PROCESSING ……....63

3.8 NETWORK PROPERTIES WITH INTRACELLULAR RECORDINGS ...…….67

3.9 WORK IN PROGRESS AND FUTURE PERSPECTIVES ……..70

4. DISCUSSION……..75

4.1 ES CELLS AS SOURCE OF NEURONS AND PROTOCOLS FOR NEURONAL DIFFERENTIATION OF ES CELLS ……75

4.2 MATURATION AND SURVIVAL OF ES-DERIVED NEURONS AND CELLULAR HETEROGENEITY……78

4.3 MEA AND NETWORK PROPERTIES OF ES-DERIVED NEURONS ……81

4.4 FUTURE PERSPECTIVES WITH ES-DERIVED NETWORKS ……83

5. REFERENCES……84

Declaration

All the work on ES cells presented in this thesis arises from my own experiments with the exception of data analysis performed in collaboration with Paolo Bonifazi and Frederic Broccard, intracellular recordings in collaboration with Giulietta Pinato and atomic force microscopy in collaboration with Marco Lazzarino.

Most of the results presented in this thesis were published in the following paper:

Jelena Ban, Paolo Bonifazi, Giulietta Pinato, Frederic D. Broccard, Lorenz Studer, Vincent Torre and Maria Elisabetta Ruaro:
Embryonic stem cell-derived neurons form functional networks *in vitro*.
Stem Cells. 2007 Mar;25(3):738-49. Epub 2006 Nov 16.

ABBREVIATIONS

ES: embryonic stem

ICM: inner cell mass

LIF: leukemia inhibitory factor

EBs: embryoid bodies

MEFs: murine embyonic fibroblasts

NSCs: neural stem cells

FCS: fetal calf serum

RA: retinoic acid

SDIA: stromal cell-derived inducing activity

FGF: fibroblast growth factor

BMP: bone morphogenetic protein

SHH: sonic hedgehog

BDNF: brain-derived neurotrophic factor

GABA: γ-aminobutyric acid

TH: tyrosine hydroxilase

MAP2: microtubule-associated protein 2

CaMKII: calcium/calmodulin dependent protein kinase II

VGLUT: vesicular glutamate transporter

GFAP: glial fibrillary acidic protein

MEA: multielectrode array

AP: action potential

PSTH: peristimulus time histogram

AFR: average firing rate

1. INTRODUCTION

The main goal of this work was to obtain neurons derived from embryonic stem (ES) cells as an alternative source to primary cell cultures where neurons are obtained from newborn or adult animals. The most important issue that we wanted to investigate was if the ES-derived neurons can form functional neuronal networks, since at that point, in the literature there were no available data about ES-derived neuronal networks.

1.1 STEM CELLS - SOME GENERAL INFORMATION

Stem cell is the name given to cells with broad differentiation potential that retain the capacity for self-renewal indefinitely (Baizabal et al, 2003; Keller, 1995).

Stem cells have varying differentiation potential. The fertilized oocyte (the zygote) and the descendants of the first two divisions are *totipotent* cells, that is able to form the embryo and the trophoblasts of the placenta. After about 4 days, these totipotent cells begin to specialize, forming a hollow ball of cells, the blastocyst, and a cluster of cells called the inner cell mass (ICM) from which the embryo develops. The ICM cells are considered to be *pluripotent*, able to differentiate into all cells that arise from the three germ layers, but not the embryo, because they are unable to give rise to the placenta and supporting tissues (Alison et al, 2002; Bishop et al, 2002; Gottlieb, 2002).

Differentiation potential decreases during development: cells that will form different tissues and organs are able to differentiate into a limited range of cell lineages (appropriate to their location). These cells are *multipotential* stem cells. For example, the

central nervous system (CNS) stem cells have a tri-lineage potential capable of generating neurons, oligodendrocytes, and astrocytes.

Finally we have *unipotential* stem cells, capable of self-renewal and generation of only one specific cell type. For example, epidermal stem cells in the basal layer produce only keratinized squames (Alison et al, 2002).

Terminally differentiated cells cannot divide, so most of the adult tissues and organs have their specific stem cells responsible for growth and regeneration, i.e. after injury. Since the plasticity decreases with developmental age, fetal stem cells are significantly more plastic than their adult counterparts (Kennea and Mehmet, 2002).

The cells used in this study, derived from ICM of mouse embryo, are called **embryonic stem (ES) cells** and can be grown *in vitro*, maintaining their self-renewal capacity and pluripotency.

1.2 DISCOVERY OF ES CELLS

ES cells were first isolated in 1981 by Gail Martin and Martin Evans, independently (Martin, 1981; Evans and Kaufman, 1981). Before that, the *in vitro* models for the study of the embryonic development were embryonic carcinoma cell (ECC) lines, derived from teratocarcinomas (tumors that arise with relatively high efficiency when mouse embryos are transplanted to an extra-uterine site in a histocompatible host). ES cells were derived from ICMs cultured in ECC-conditioned medium and retained all the essential features of teratocarcinoma stem cells: they were diploid, capable of tumor

formation when injected in athymic mice, pluripotent and capable of differentiation *in vitro* (Martin, 1981).

1.3 PROPERTIES OF ES CELLS

The most relevant features of ES cells are:

- high proliferation and self-renewal capacity

ES divide without limit: they can propagate indefinitely in an undifferentiated state. Even after 140 cycles of division, they remain genetically normal. Why ES cells have this natural immortality has not been understood in detail yet. This unlimited replication potential may be related to the extremely low level of genomic DNA methylation that has an important role in epigenetic gene silencing and maintenance of genome stability, and even triple knockout ES cells lacking all 3 enzymes involved in DNA methylation still retain high proliferation rate (Tsumura et al, 2006). ES cells also maintain a high level of telomerase activity (Armstrong et al, 2005; Bishop et al, 2002; Gottlieb, 2002; O'Shea, 1999).

- stable diploid karyotype

Mouse ES cells are genetically normal, non-transformed cells having a stable diploid karyotype (Baizabal et al, 2003; Bishop et al, 2002; Hancock et al, 2000; Martin, 1981).

- pluripotency

Pluripotency is demonstrated by transplanting ES cells to the inner cell mass of a host embryo. If the embryo is then implanted into a foster mother, it develops into an outwardly normal mouse called *chimera*, in which all tissues have cells derived from both the transplanted ES cells and the host. Thus the transplanted ES cells respond to appropriate cues and differentiate into all cell types of the normal body. Chimeric male mice are fertile and have sperm derived from ES cells (Alison et al, 2002; Baizabal et al, 2003; Gottlieb, 2002).

- wide differentiation potential *in vitro*

When provided with the appropriate signals, ES have the capacity to differentiate, presumably via formation of precursor cells, into almost all mature cell phenotypes (Bishop et al, 2002). The production of differentiated, functional progeny was obtained in many different systems: cardiomyocytes, haematopoietic cells, endothelial cells, skeletal muscle, chondrocytes, adipocytes, liver, pancreatic islets and neurons (for a review, see Keller, 2005). *In vitro* differentiation of ES cells recapitulates a number of normal developmental processes that occur in mammalian embryos (Hancock et al, 2000).

- clonability

ES cells are amenable to a wide variety of genetic manipulations. For example, a very powerful application of this culture system is to target marker genes such as lacZ, GFP, or luciferase into loci that are activated during the development of specific lineages (Baizabal et al, 2003; Friedrich and Soriano, 1991; Hancock et al, 2000; Keller, 2005;

Thomas and Capecchi, 1987; Ying et al, 2003). With the possibility to induce genetic modifications, wild-type and mutant ES cell lines can be compared (Keller, 2005; Bibel et al, 2004).

Because of these characteristics, ES cells have many and very important applications both in basic and applied research.

1.4 APPLICATION OF STEM CELL TECHNOLOGY

1.4.1 Cell replacement therapy

ES represent potential therapeutic reagents for various degenerative diseases and damaged organs. They can be transplanted in order to replace damaged/lost cells or engineered to express therapeutic genes. Type I diabetes, cardiovascular diseases, Parkinson's disease, blood cell diseases, and certain types of liver diseases are considered candidates for cell replacement therapy. Transplantation of specific ES-cell-derived cells into pre-clinical models of human disease is already underway (Barberi et al, 2007; Brüstle et al, 1999; Keller, 2005; Kim et al, 2002; Lee et al, 2007; Morizane et al, 2006; Okano, 2002; O'Shea, 1999; Perrier and Studer, 2003).

The possibility of theoretically generating an unlimited number of any kind of cell type is of particular interest to neurobiologists, as homogenous cell populations are not available in sufficient quantities for the characterization of brain neurons using biochemical approaches (Bibel et al, 2004).

Because ES are derived prior to implantation, certain immune-related cell-surface proteins (e.g., class I products of the major histocompatibility complex) are not yet expressed, which could solve the problem of donor/recipient compatibility and rejection of transplants (O'Shea, 1999).

1.4.2 Developmental biology

ES cells provided the basis for establishing an *in vitro* model of early mammalian development. They can both generate and respond *in vitro* to signals that normally regulate murine development (Fraichard et al, 1995). ES cells have been used to isolate unique genes involved in cell-type specific differentiation and to study the cascade of gene expression during the development of a particular lineage or tissue (O'Shea, 1999).

Cell culture studies on non-human embryonic stem cell differentiation will help to guide the development of methods that can be applied to human ES cell studies. The wide range of powerful genetic manipulations that are possible in ES cells allow the performance of a series of experiments that would be difficult or impossible in primary cell cultures or in immortalized cell lines (Hancock et al, 2000).

1.4.3 Drug discovery

In addition to developmental biology and cell-based therapy, the ES cell model has widespread applications in the areas of drug discovery and drug development. With respect to drug development, cell types such as cardiomyocytes and hepatocytes generated from human ES cells could provide ideal populations for predictive toxicology.

These human cells could reveal the toxicity of certain drugs that might not be detected using conventional assays that rely on animal models (Keller, 2005).

1.5 CULTURE OF ES CELLS

ES cells are derived from mouse, primates and humans (Evans and Kaufman 1981; Martin, 1981; Thompson et al, 1985 and 1988).

ES cells were initially established and maintained by coculture with mouse embryonic feeder cells. Feeder cells such as murine embryonic fibroblasts (MEFs) serve as a basal layer for stem cells and provide secreted factors, extracellular matrix, and cellular contacts for the maintenance of stem cells in an undifferentiated state without losing pluripotency.

Subsequent studies identified **leukemia inhibitory factor (LIF)** as one of the feeder-cell-derived molecules that plays a pivotal role in the maintenance of mouse ES cells. In the presence of appropriate batches of fetal calf serum (FCS), recombinant LIF can replace the feeder cell function and support the growth and survival of undifferentiated mouse ES cells. However, LIF does not have the same effect on human ES cells and appear to play no role in their self-renewal (Keller, 2005).

Molecular analyses have revealed that LIF functions through the gp130 activation of signal transducer and activator of transcription STAT3. In addition to STAT3, two other transcription factors, Oct3/4 and nanog, have been shown to play pivotal roles in maintaining the undifferentiated state of ES cells (Keller, 2005).

When LIF or feeder cells are withdrawn and ES cells are cultured on a nonadhesive substrate, most types of ES cells form floating aggregates known as **embryoid bodies (EBs)** that grossly resemble early embryos: endoderm exterior, mesoderm and ectoderm interior, surrounding a large cystic yolk sac-like cavity.

If plated on adhesive substrates in the absence of added factors, EBs give rise to a complex mixture of terminally differentiated cells including heart, muscle, blood, and neurons among others (Bishop et al, 2002; Gottlieb, 2002).

Exposure to different agents (retinoic acid (RA), dimethyl sulfoxide (DMSO), hexamethylene bisacetamide (HMBA)), growth factors and cytokines (LIF, tumor necrosis factor-α (TNF-α), activin A, bone morphogenetic protein (BMP)-2,4, insulin, nerve growth factor (NGF), basic fibroblast growth factor (bFGF), ciliary neurotrophic factor (CNTF), T3) and panels of haematopoietic growth factors were used with the aim of inducing/modifying differentiation or of examining alterations in gene expression induced by these agents, with mixed results (O'Shea, 1999).

In a defined medium, in the absence of signaling molecules, ES differentiate into neuroepithelium-like cells, as determined by expression of Pax 6. ES themselves express a number of growth factors and cytokines (including inhibin, follistatin, and fibroblast growth factors) and their receptors, which are altered with differentiation (O'Shea, 1999).

Because of their origin from the inner cell mass/early epiblast, it has been stated that ES cells mostly resemble ectodermal tissue: in fact, ES cells do express many structural genes (intermediate filament proteins, extracellular matrix proteins, cell adhesion molecules) expressed by primitive ectoderm (O'Shea, 1999).

1.6 ES CELLS AND NEURONAL DIFFERENTIATION

Neuronal differentiation is an early event in mammalian embryogenesis that occurs soon after germ layer differentiation and it is thought to be determined during gastrulation (E6.5~E8) (Kawasaki et al, 2000).

The tissues of the CNS are derived from a clearly defined neuroectoderm, the neural plate, which lies along the dorsal midline of the embryo. It appears that the neural plate arises by the local suppression or avoidance of signals that induce non-neuronal differentiation. Both the intrinsic factors and the extrinsic soluble signals affect the regional patterning and specific neuronal differentiation. Neuronal fate is suppressed by bone morphogenetic proteins (BMPs) and, *in vivo*, several molecules that promote neuronal differentiation such as noggin, follistatin, chordin, and sonic hedgehog (SHH) are BMP antagonists (Kennea and Mehmet, 2002).

An intrinsic characteristic of the nervous system is its enormous cellular diversity. In the adult brain, specific neurons produce specific neurotransmitters and receptors and make specific contacts with other cells. Neural stem cells (NSCs) are the source of all types of neurons: they appear during neural plate formation and possibly constitute the major cell type of early ectoderm (Baizabal et al, 2003).

Fetal NSCs have a typical radial morphology and are known in general as radial glia (Okano, 2002). As development progresses, the neural tube forms and NSCs become progressively less abundant and more restricted progenitor cells emerge (Baizabal et al, 2003).

The common underlying concept is that NSCs are organ stem cells present in the CNS that can give rise to themselves in a self-replicating capacity, as well as to astrocytes, oligodendrocytes, and neurons. The multilineage potential of NSCs is at least partly mediated by the generation of cell lineage-restricted intermediate progenitor cells that produce only neurons (neuronal progenitor cells) and glial progenitor cells that produce only astrocytes or oligodendrocytes. Thus, the cellular diversity of the CNS is likely to be generated in a stepwise fashion (Okano, 2002).

CNS stem cells have a tri-lineage potential capable of generating neurons, oligodendrocytes, and astrocytes. During CNS development, neurons are generated first, then glia (Kennea and Mehmet, 2002).

When most nervous system structures are defined, complex migration and differentiation patterns initiate, followed by guided axonal growth that finally allows specific cell targeting, thus defining the stereotypical neuronal wiring of the nervous system (Baizabal et al, 2003).

The mammalian brain was long believed to be an exceptional organ with very low turn-over and poor regenerative capacity of neuronal cells. It has been recently shown that adult brain cells exhibit the capacity to both self-renew and generate differentiated progeny *in vitro* and *in vivo*. Neurogenesis in the adult mammalian brain has been identified in two main areas of the adult brain: subventricular zone (SVZ) and the hippocampus (Baizabal et al, 2003; Kennea and Mehmet, 2002; Okano, 2002).

1.7 PROTOCOLS FOR NEURONAL DIFFERENTIATION OF ES CELLS

During the last decade, many different protocols have been developed to promote neuronal differentiation from ES cells *in vitro*. Each of the three major neuronal cell types of the central nervous system — neurons, astrocytes, and oligodendrocytes — can be derived, and relatively pure populations of each type can be isolated when cultured under appropriate conditions (Okabe et al, 1996; Barberi et al, 2003). In addition to the generation of these different neuronal populations, some differentiation procedures allow the selective derivation of specific neuronal subtypes (Barberi et al, 2003; Bibel et al, 2004; Lee et al, 2000; Li et al, 1998; Morizane et al, 2002; Westmoreland et al, 2001).

The protocols for differentiation to specific types of neurons have included the sequential combination of regulators (cytokines and growth factors) that are known to play a role in the establishment of these lineages in the early embryo (Keller, 2005). For instance, midbrain dopaminergic neurons have been generated in the EBs system by overexpression in the cells of the transcription factor nuclear-receptor-related factor1 (Nurr1), and the addition to the cultures of SHH and FGF8 (Kim et al, 2002). Nurr1, SHH, and FGF8 are required for the development of this class of neurons in the early embryo. More recent studies have demonstrated the development of cholinergic, serotonergic, and GABAergic neurons in addition to dopaminergic neurons, when differentiated on MS5 stromal cells in the presence of different combinations of cytokines (Barberi et al, 2003; Keller, 2005).

Despite the use of growth factors favoring differentiation of a particular cell type, the resulting ES-derived cultures were heterogeneous. None of the approaches used on murine ES cells has yet been shown to give 100% yield of cells with the required phenotype, so methods to purify the populations are required (Evans et al, 2006; O'Shea, 1999).

The protocols for neuronal differentiation of ES cells can be grouped into three different approaches:

1. retinoic acid treatment (Bain et al, 1995; Fraichard et al, 1995)
2. V stages protocol or selective method (Bibel et al, 2004; Hancock et al, 2000; Lee et al, 2000; Okabe et al, 1996; Westmoreland et al, 2001)
3. stromal cell-derived inducing activity (SDIA) (Barberi et al, 2003; Kawasaki et al, 2000; Morizane et al, 2002)

1. retinoic acid treatment

This protocol involves the formation of embryoid bodies (EBs) and the addition of retinoic acid (RA). When RA-induced EBs are dissociated and plated on an adhesive substrate, cells differentiate further into neurons, astrocytes, and oligodendrocytes (Bain et al, 1995; Finley et al, 1996; Strübing et al, 1995). Approximately 70% of the neurons are glutamatergic, 25% GABAergic, and 5% glycinergic. Other protocols utilizing RA but differing in detail (Fraichard et al, 1995) produce also cholinergic neurons (from 10 to 20% of the total neuronal-like cell population). After 20 days, other differentiated cells

overgrow and neuron-like cells progressively disappear, in particular glial cells are no longer detectable.

Advantages/disadvantages of the method

The simplicity of the method and the strong induction of neuronal differentiation are the main advantages. Nevertheless, RA is a strong teratogen, is supposed to perturb neuronal patterning and neuronal identities in EBs as it does *in vivo*. For instance, RA treatment of early embryos causes suppression of forebrain development. It is therefore preferable to avoid RA treatment for therapeutic applications or basic neuroscience research unless RA induces the particular type of neurons of interest for a specific study (Kawasaki et al, 2000).

2. V stages protocol

This protocol involves several steps: the formation of EBs (stage 2), their subsequent plating on an adhesive substrate in serum-free medium to select for neuronal precursors (stage 3), the proliferation of precursors in the presence of mitogen, basic fibroblast growth factor (bFGF; stage 4), and the differentiation induction by removal of the mitogen (stage 5; Lee et al, 2000). Withdrawal of bFGF triggers differentiation into a mixture of neurons (>60% after 1 week of differentiation) and glial cells (10-15%). Glutamatergic and GABAergic neurons are obtained, but cholinergic neurons and oligodendrocytes are not observed (Okabe et al, 1996). Westmoreland et al (2001) obtained 51% neurons, 45% of which were GABAergic. It is also possible to expand

cryopreserved neuronal progenitor. After freezing, more than 50% of the cells retain viability and differentiate (Hancock et al, 2000).

Bibel et al (2004) used this method in combination with RA treatment: after 1 week of differentiation, 93% of the neurons are glutamatergic while less than 1% are GABAergic, dopaminergic and cholinergic.

Advantages/disadvantages of the method

The differentiation using EBs offers the advantage of providing a three-dimensional structure that enhances cell–cell interactions that may be important for certain developmental programs. The complexity of the EBs can also be a disadvantage because they contain increased number of endodermal and mesodermal derivatives and this inherent heterogeneity makes identification and control of factors involved in specific NSC differentiation rather difficult (Kawasaki et al, 2000; O'Shea, 1999).

3. SDIA

This approach includes the culture of ES cells on stromal (or mesenchymal) cells that promote neuronal differentiation when used as feeders (without inducing mesodermal markers). This neuronal-inducing activity was named stromal cell-derived inducing activity (SDIA) (Kawasaki et al, 2000; Morizane et al, 2002).

The SDIA method does not involve EBs formation or RA treatment, and each differentiating colony grows from a single ES cell in two dimensions under serum-free conditions. SDIA method mimics the time course of early development of the midbrain:

for instance, tyrosine hydroxilase (TH) positive dopaminergic neurons appear on induction days 6–8, while TH is first detected in the fetal mouse midbrain on E11.5. Given that ES cells behave like the inner cell mass (E4), and that the neuronal fate is determined during gastrulation (E6.5-E8) period, the expression required for TH induction *in vitro* correlates well to that seen in the embryo (Kawasaki et al, 2000; Morizane et al, 2002).

The molecular nature of SDIA is still unknown (Kawasaki et al, 2000; Morizane et al, 2006) and is though to be due to membrane-bound factor(s) and/or soluble factor(s) secreted from stromal cells.

On induction day 12, neurons represent 52% of total cells: 16% are dopaminergic, 18% GABAergic, 9% cholinergic and 2% serotonergic (Kawasaki et al, 2000). Morizane et al (2002) obtained 20-30% of dopaminergic neurons, which represented 40-50% of SDIA-treated cells. The percentage of dopaminergic neurons is higher in respect to other methods.

Barberi et al (2003) improved the protocol for the selective generation of dopaminergic, serotonergic, cholinergic, GABAergic and motor neurons, as well as neural stem cells (NSCs), astrocytes and oligodendrocytes.

Advantages/disadvantages of the method

The SDIA method is technically simple, and the induction is efficient and fast. Coculture with stromal cells provides the beneficial growth promoting effects of the particular cell line used. This method allows rapid and efficient derivation of most central nervous system phenotypes. The regional fate specification can be controlled by

manipulation of external medium conditions and by sequential patterning cues that seem to recapitulate *in vivo* development. Some difficulty can be encountered when attempting to separate the ES-cell-derived cells from the stromal cells (Keller, 2005).

For our purposes, SDIA protocol offers the main advantage of selective generation of different neuronal subtypes and therefore it has been chosen for this work.

Regardless of the protocol used, differentiation of ES cells into neurons has been followed by examining morphology (establishment of the neuronal polarity and separation into axonal and dendritic compartments) and the expression of neuron specific markers including neurofilament proteins, neuronal tubulin, microtubule-associated protein-2 (MAP-2, the dendrite specific marker), growth-associated protein-43 (GAP-43; specific axonal marker), Tau, neurocan, Wnt 1 and MASH1. Vesicular glutamate transporter 2 (VGLUT2) and Ca2+/calmodulin dependent protein kinase II (CaMKII) were used to mark glutamatergic neurons. To mark different subtypes of neurons, enzyme proteins involved in biosynthesis of neurotransmitters like glutamic acid decarboxylase (GAD) for GABAergic, acetylcholinesterase (AchET) and choline acetyltransferase (ChAT) for cholinergic, and tyrosine hydroxilase (TH) for dopaminergic neurons were used. Alternatively, dopaminergic neurons can be revealed by measuring the release of dopamine directly by RP-HPLC (Barberi et al, 2003; Lee et al, 2000).

Glial differentiation has been monitored by the expression of the glial fibrillary acidic protein (GFAP), OP4 (for astrocytes), and Gal C and O4 (for oligodendrocytes).

The intermediate filament protein nestin and Pax 6 have been employed to mark neuronal precursors.

The generation of synapses was investigated by examining the presence of synaptic vesicles and specific synaptic proteins like synapsin, synaptic vesicle protein 2 (SV2), synaptophysin, and synaptotagmin.

1.8 INTRACELLULAR RECORDINGS OF ES-DERIVED NEURONS

Functional differentiation of ES-derived neurons obtained with different protocols was investigated with the aim to determine whether cells are electrically excitable when examined using whole-cell patch-clamp (Bain et al, 1995; Bibel et al, 2004; Finley et al, 1996; Fraichard et al, 1995; Hancock et al, 2000; Jügling et al, 2003; Lee et al, 2000; Miles et al, 2004; Nakayama et al, 2004; Okabe et al, 1996; Strübing et al, 1995).

Electrophysiological data from ES-derived neurons obtained with different protocols validate their functional differentiation as well as the formation of synapse between ES-derived neurons (Miles et al, 2004) or between an ES-derived neuron and a mature neuron in organotypic slices (Benninger et al, 2003) or *in vivo* (Lee et al, 2000; Rüschenschmidt et al, 2005; Wernig et al, 2004).

1.9 MEA AND NEURONAL NETWORKS

Systems neuroscience studies how neurons behave when connected together to form neuronal networks and how they process information (Bonifazi et al, 2005;

DeCharms and Merzenich, 1996; Georgopoulos et al, 1986; Gray et al, 1989; Hopfield, 1982; Nicolelis et al, 1998; Rumelhart and McClelland, 1998; Thorpe et al, 2001). A fundamental pre-requisite to investigate how information is processed is to monitor simultaneously the electrical activity of a large population of neurons in the networks.

In the last decade the application of new electrophysiological and optical techniques *in vivo* (Kerr et al, 2005; Nicolelis et al, 1997; Stosiek et al, 2003) allowed to characterize better the functional properties of neuronal networks giving the possibility to study neural coding mechanisms and distributed representations in different parts of the brain. In this way, it was shown how information can be encoded in the firing rate of an ensemble of neurons or in the synchrony of firing (Gray et al, 1989; Singer and Gray, 1995), in the relative timing of action potentials (APs) (DeCharms and Merzenich, 1996; Hopfield, 1995; O'Keefe and Recce, 1993) or in the latency of first evoked APs (Johansson and Birznieks, 2004; Thorpe et al, 2001). However, due to the variability of the experimental conditions and the intrinsic complexity of the investigated system, it is very difficult to obtain a detailed analysis if performed *in vivo*. Many of these problems are bypassed by studying neuronal networks in *in vitro* cultures where experimental conditions and properties can be controlled in a more reliable way.

When neurons are isolated and plated on an appropriate substrate, they readily grow forming axo-dendritic arborization extending up to some millimeters and covered by a large number of functional synapses (Marom and Shahaf, 2002; Potter, 2000; Van Pelt et al, 2005). Distribution and cell types present in cultures are similar to those found *in vivo* (Neale et al, 1983; Huettner and Baughman, 1986; Nakanishi and Kukita, 2000) and, although they have lost the original connectivity of the intact tissue, they represent a

good system to study how neuronal networks operate as a whole under controlled conditions. Cultures with random connections, provide a more general view of neuronal networks and assemblies, not depending on the circuitry of a neuronal network *in vivo*, and allow a more detailed and careful experimental investigation (Bonifazi et al, 2005).

Multielectrode arrays (MEAs) represent a unique tool to investigate network dynamics allowing the recording of the electrical activity of neuronal networks both in space and time (Morin et al, 2005). On MEAs cells can be cultured for several weeks or even months (long-term cultures). The interaction among several cells in culture can be studied by measuring extracellularly and simultaneously the electrical activity of these cells (multi-site recordings) and it is also possible to stimulate and record their evoked electrical activity.

Moreover, the chronic monitoring and stimulation of *in vitro* preparations for long-term periods provides a unique way to investigate developmental and plasticity mechanisms in a variety of systems and have been widely used to characterize the spontaneous and the evoked activity of neuronal networks (Bonifazi et al, 2005; Jimbo et al, 1992 and 1999; Kamioka et al, 1996; Maeda et al, 1995; 1998; Potter, 2000; Robinson et al, 1993 a and b; Ruaro et al, 2005; Shahaf and Marom, 2001; Van Pelt et al, 2004 and 2005; Welsh et al, 1995).

Even if it has been shown that ES cells or ES-derived neuronal precursors can incorporate into the nervous system where they can differentiate into neurons and glia (Brüstle et al, 1999; Hara et al, 2004; McDonald et al, 1999; Wernig et al, 2004), little is known on the capability of ES-derived neurons to form functional networks and on their

properties. Since the main function of neurons is communication, we decided to test the ability of ES-derived neurons to form functional networks and in particular to process information in a reliable way.

2. MATERIALS AND METHODS

2.1 Reagents and Media

Fetal Calf Serum (FCS) was from Euroclone, Leukemia inhibitory factor (ESGRO-LIF) from Chemicon, all the recombinant proteins (bFGF, FGF8, SHH, BDNF, NT4) were from R&D Systems, Mitomycin C, laminin, HBSS and HEPES were from Sigma and all other reagents and media were from Gibco-Invitrogen.

2.2 ES-derived neuronal differentiation

ES cells were induced to differentiate into neurons using the protocol for GABAergic neurons described in Barberi et al (2003), with some modifications. Undifferentiated BF1/lacZ ES cells were grown on murine embryonic fibroblast feeder in ES medium (Knockout Dulbecco's modified eagle medium (D-MEM) supplemented with 15% FCS, 0.1 mM non essential amino acids, 50μM β-mercaptoethanol, 2 mM L-alanyl-L-glutamine (Glutamax), 100 U/ml penicillin, 100 μg/ml streptomycin and 2000 U/ml of LIF) and replated every tree or four days. Stromal cells (MS5) were grown in α-MEM medium (α-minimal essential medium (α-MEM) containing 10% FCS, 2 mM L-alanyl-L-glutamine (Glutamax), 100 U/ml penicillin and 100 μg/ml streptomycin) and replated every 2-3 days at 70% confluency. For the neuronal differentiation, MS5 were grown to 100% confluency (contact inhibition induced growth arrest) and treated with 1μg/ml Mitomycin C overnight. The next day, Mitomycin C was washed, ES trypsinized, and

plated on Mitomycin C treated-MS5 cells as single-cell suspension at a density of 250 cells/cm^2 in KSR medium (Knockout D-MEM supplemented with 15% knockout serum replacement, 0.1 mM non essential amino acids, 50μM β-mercaptoethanol, 2 mM L-alanyl-L-glutamine (Glutamax), 100 U/ml penicillin and 100 μg/ml streptomycin) and cultured for 6 days. The KSR medium was changed every day. The ES-derived epithelia structures were then mechanically separated from MS5 cells monolayer, by incubating the cells with Hank's balanced salt solution (HBSS) supplemented with 0.15 M Hepes for 5 minutes and flushing through the pipette tip near the colony without removing MS5 feeder. The detached ES cells colonies were resuspended with KSR medium and plated on 15μg/ml polyornithine- 1μg/ml fibronectin-coated dishes. After 2-3 hours the medium was changed with N2 medium (DMEM-F12 supplemented with 1.55 g/l (8.6mM) glucose, 2 g/l (23.8mM) sodium hydrogen carbonate, 25 mg/l insulin, 100 mg/ml human apo-transferrin, 100μM putrescine, 30nM sodium selenite, 20nM progesterone, 100 U/ml penicillin and 100 μg/ml streptomycin) containing 10ng/ml basic fibroblast growth factor (bFGF) and 1μg/ml fibronectin (amplification medium) and cells were induced to proliferate in presence of bFGF for 4 days. During the last 2 days 200ng/ml of Sonic Hedgehog (SHH) and 100ng/ml fibroblast growth factor (FGF) 8 were added as patterning factors. Cells were then trypsinized and plated on 15μg/ml polyornithine-1μg/ml laminin-10% FCS in N2 medium-coated MEA plates or glass coverslips in N2 medium containing 10% FCS, 10ng/ml BDNF, 10ng/ml NT4, and 1μg/ml laminin (differentiation medium). Half of the differentiation medium was then changed twice a week. The post mitotic neurons were maintained in culture up to 10 weeks.

2.3 Hippocampal culture preparation

Hippocampal neurons from Wistar rats (P0-P2) were prepared as previously described (Ruaro et al, 2005). Cells were plated on polyorhitine-matrigel-coated MEA (Ruaro et al, 2005) at a concentration of 8 x 10^5 cells/cm^2 and maintained in Minimal Essential Medium with Earle's salts (Gibco) supplemented with 5% FCS, 0.5% D-glucose, 14 mM Hepes, 0.1 mg/ml apo-transferrin, 30 μg/ml insulin, 0.1 μg/ml D-biotin, 1 mM vitamin B12, and 2μg/ml gentamycin. After 48 hours, 5 μM cytosine-β-D-arabinofuranoside (Ara-C) was added to the culture medium to block glial cell proliferation. Half of the medium was changed twice a week. Neuronal cultures were kept in an incubator providing a controlled level of CO_2 (5%), temperature (37^{o}C) and moisture (95%). In all experiments, hippocampal cells were used after 3 weeks in culture.

2.4 Immunocytochemistry

Cells were fixed in 4% paraformaldehyde containing 0.15% picric acid in phosphate-buffered saline (PBS), saturated with 0.1 M glycine, permeabilized with 0.1% triton X-100, saturated with 0.5% BSA in PBS and then incubated for 1h at room temperature (20-22°C) with primary antibodies. The primary antibodies were: a) rabbit polyclonal antibodies- against GABA, serotonin, CaMKII (all from Sigma), TH (Pel Freeze); b) mouse monoclonal antibodies- TUJ1 (Covance), MAP2 (Sigma), GFAP (Sigma), nestin (Chemicon), O4 (Chemicon), SMI-94 (anti-MBP, Covance); c) guinea pig polyclonal antibody against V-GLUT2 (Chemicon); D) goat polyclonal antibody against ChAT (Chemicon). The secondary anti-mouse-FITC and anti-rabbit-RITC antibodies were from

Sigma, goat anti-mouse IgG_1-FITC and IgG_{2a}-TRITC were from Southern Biotech, anti-guinea pig-488 Alexa and anti-goat-594 Alexa were from Molecular Probes. Total nuclei were stained with 2µg/ml in PBS Hoechst 33342 (Sigma).

Alexa Fluor 488 phalloidin was used to mark F-actin (Molecular Probes). The incubation time was 30 min at room temperature (20-22°C).

The cells were examined using a fluorescence (Zeiss Axiovert 2) and confocal (Leica DMIRE2) microscope equipped with differential interference contrast (DIC) and phase-contrast optics. Digital images were acquired with a CCD camera (Zeiss), cells were selected on the screen and counted with with Image J Cell Counter Software. Data values are presented as the means +/- SD. All results were derived from at least three independent experiments.

2.5 Atomic force microscopy

Atomic Force Microscopy (AFM) was performed using a commercial AFM (Nanowizard II, JPK Berlin) combined with an inverted optical microscope (Zeiss Axiovert 200), and a fluorescence set-up (Zeiss X-cite). AFM was operated in contact mode in liquid, adjusting the contact force during imaging to minimize the force exerted by the tip on the sample during scanning. Soft tips from VEECO with low force constant (OBL, 0.03N/m) were utilized and forces were kept between 100pN and 1nN during scanning. AFM and optical images were superimposed using commercial Software (DirectOverlay, JPK, Berlin) that corrects the optical aberrations using the AFM scanner position sensors with an accuracy better than 1nm.

To perform AFM analysis, ES cells were grown and on 24mm diameter glass coverslips, mounted into the AFM liquid cell, immersed in PBS buffer and mounted into the AFM microscope. After laser alignment and tip calibration, the system was left to settle for a couple of hours with laser and microscope condenser on, to minimize thermal drift and force drift during image acquisition.

Image post processing (JPK Image processing, Berlin) was minimized in order to not add image processing artifacts.

2.6 Electrophysiological recordings

Dissociated hippocampal and ES-derived neuronal cultures were transferred in a recording chamber, perfused in Ringer's solution (145mM NaCl, 3mM KCl, 1.5mM $CaCl_2$, 1mM $MgCl_2$, 5mM glucose, 10mM Hepes, adjusted to pH 7.3 with NaOH) and visualized with an upright microscope (Olympus) with DIC optics. Patch-clamp recordings were performed with an Axoclamp 2-B amplifier (Axon Instruments). Experiments were performed at room temperature (20-22°C). Electrodes were pulled (Narishige) and filled with an intracellular solution containing: 120mM potassium-gluconate, 10mM sodium-gluconate, 10mM Hepes, 10mM sodium-phosphocreatine 10, 4mM MgATP, 4mM NaCl, 2mM Na_2ATP and 0.3mM Na_3GTP (adjusted to pH 7.3 with KOH): in these conditions the electrode resistance was 15-20 MΩ. To enhance the driving force for chloride currents, some experiments were performed in symmetrical chloride conditions by substituting potassium-gluconate with KCl in the pipette solution; in these conditions the resistance of the electrodes was 5-10 MΩ. The data were digitized

at 20 kHz (Digidata 1200, Axon Instruments) and analyzed using pClamp9 software (Axon instruments). Values of membrane potentials were corrected for the effects of liquid junction potential during seal formation.

Pharmacological identification of postsynaptic responses was performed by application of the following synaptic blockers: 30μM D-AP5, 20μM 6-cyano-7-nitroquinoxaline-2,3-dione (CNQX); 10μM SR-95531 (gabazine). All reagents were purchased from Tocris.

2.7 MEA electrical recordings and electrode stimulation

ES-derived neurons cultured on MEAs, were kept in an incubator with a controlled level of CO_2 (5%), temperature (37°C) and moisture (95%). Before electrical recordings, dishes were sealed with a cap distributed by MultiChannel Systems (MCS) to reduce gas exchange and eliminate evaporation and contamination and transferred from the culture incubator to a different incubator with controlled CO_2 (5%), and temperature (37°C) where the electrical recording system was placed. Before starting the recordings, the neuronal culture was allowed to settle for approximately 30 minutes. After termination of the experiment, usually after 2-3 hours, the medium was changed, and the dish was moved back to the incubator.

MCS commercially supplied the multi electrode array (MEA) system used for electrophysiology. MEA dishes had 10x6 TiN electrodes with an interelectrode spacing of 500 μm and each metal electrode had a diameter of 30 μm. The MEA is connected to a 60-channel, 10 Hz – 3 kHz bandwidth pre-amplifier/filter-amplifier (MEA 1060-AMP) which redirects the signals toward a further electronic processing (i.e. amplification and

analog to digital (AD) conversion), operated by a high performance computer. Signal acquisitions are managed under software control, and each channel was sampled at a frequency of 20 kHz. One electrode was used as ground. Sample data were transferred in real time to the hard disk for off-line analysis. Each metal electrode could be used either for recording or for stimulation. The voltage stimulation used consisted of bipolar pulses lasting 100 μs at each polarity, of amplitude varying from 200mV to 900mV, injected through a single channel of the STG1004 Stimulus Generator (Wagenaar et al, 2004). The voltage pulse generated by the STG1004 was applied in parallel with the set of electrodes manually selected for stimulation (simultaneous multisite stimulation). An artifact lasting 5–20 ms, caused by the electrical stimulation, was induced on the recording electrodes but was removed from the electrical recordings during data analysis (Ruaro et al, 2005; Wagenaar and Potter, 2002). For each stimulus the culture was stimulated for 100 trials every 4 seconds.

2.8 Data analysis

Acquired data were analyzed using MATLAB (The Mathworks, Inc.). For each individual electrode, we computed the SD (σ) of the noise, which ranged from 3 to 6 μV, and only signals crossing the threshold of -5σ were counted as APs and used for data analysis. AP sorting was obtained by using principal component analysis and open source toolboxes for the analysis of multielectrode data (Egert et al, 2002) with MATLAB. To quantify the amount of small amplitude spikes, a fixed threshold of -50 μV was used, and the number of APs recorded was then compared with that obtained with a threshold of -

5σ. The firing rate (FR(t)) of Fig. 14B and the probability distribution of the number of spikes per bin of Fig. 15A and B were computed by counting the number of spikes recorded by the whole MEA in time bins of 250 ms. To compute the average firing rate (AFR) of the neurons, peristimulus time histograms (PSTHs) were calculated for the sorted neurons (Fig. 18A and C) using a 10 ms time bin, where time 0 ms corresponds to the delivery of the stimulation. Similarly, when APs recorded by the whole array of electrodes were pooled, the array PSTH (APSTH) was calculated (Fig. 18B and D). The coefficient of variation (CV) of any variable analyzed is the SD over the mean of the variable. To test the difference of firing between the spontaneous activity and the activity after the extracellular stimulation, we considered the number of APs, respectively, in the 50 ms preceding and in the 50 ms after the stimulus. To test the significant difference in the variation between the two quantities we used one-way analysis of variance (ANOVA).

2.9 Calculation of the mutual information

With the aim of decoding the stimulus intensity, we considered the array response (AR_t). We used information theory (Shannon and Weaver, 1949) and, in particular, mutual information to estimate the amount of information that can be decoded in different time bins (i.e., varying *t*) and for different extents of pooling (i.e., different number of electrodes). In particular, the mutual information was calculated as follows:

$$I_t \equiv I_t(R,S) = \sum_{s\in S} p(s) \sum_{r\in R} p_t(r \mid s) \cdot \log_2 (p_t(r \mid s) / p_t(r))$$

where

$$p_t(r) = \sum_{s \in S} p(s) \cdot p_t(r \mid s)$$

I_t quantifies in bits the amount of information that a single response, r, (i.e., AR_t,) provides about the intensity of the stimulus, s. $p_t(r)$ is the total probability of observing the response r considering the time bin 0 to t ms after the stimulus, averaged over all stimuli. In our case, all stimuli occurred with equal probability, $p(s)$. In order to minimize the effects of finite sample size on our estimates of information, the real response r has been binned into different intervals, following the methods of Panzeri and Treves (1996).

2.10 Calculation of correlation

The degree of correlation of firing in the network was measured comparing the multiunit recordings of pairs of electrodes. The spontaneous activity was recorded for approximately 30 minutes and, to convert it into a time series (SA_1, …, SA_n), it was binned into firing rate with a bin width Δt. For each pair of electrodes (i, j), the cross-correlation $\rho_{i,j}$ between the time series (SA_{i1}, …, SA_{in}; SA_{j1}, …, SA_{jn}) was calculated according to the equation:

$$\rho_{i,j} = \frac{\sum_{n=1}^{N} (SA_{in} - < SA_i >)(SA_{jn} - < SA_j >)}{\sqrt{(\sum_{n=1}^{N} (SA_{in} - < SA_i >)^2)(\sum_{n=1}^{N} (SA_{jn} - < SA_j >)^2)}}$$

and the average cross correlation $< \rho >$ over all the possible pairs of electrodes was calculated. The cross-correlation analysis for the spontaneous activity shown in Figure 15 was obtained varying the size of the bin width Δt.

3. RESULTS

The goal of this work was to find the appropriate protocol for ES differentiation into neurons in order to analyze their capability to form functional network. To study the properties of these networks, we used extracellular recordings on multielectrode arrays (MEAs), so it was essential to develop the optimal conditions to grow and differentiate neurons on the MEA dishes. We selected a starting protocol for differentiation considering also the possibility to modify the network properties by changing the composition of the culture like, for example, changing the proportions of excitatory and inhibitory neurons. We opted for the protocol originally developed by Barberi et al (2003) that allows enrichment for different neuronal subtypes. In this work we used the protocol that enriched in GABAergic neurons and demonstrated that ES-derived neurons can form functional networks and have properties similar to those of primary adult neurons.

3.1 GROWTH AND NEURONAL DIFFERENTIATION OF ES CELLS

The protocol for neuronal differentiation used in this study involves stromal cell inducing activity (SDIA) and is a modification of that described in Barberi et al (2003). The ES cell line used was BF1/lacZ (kind gift from Dr. Studer). Undifferentiated ES cells were amplified by growth on Mitomycin C-inactivated murine embryonic fibroblasts (MEFs) feeder and in the presence of leukemia inhibitory factor (LIF) (Fig. 1).

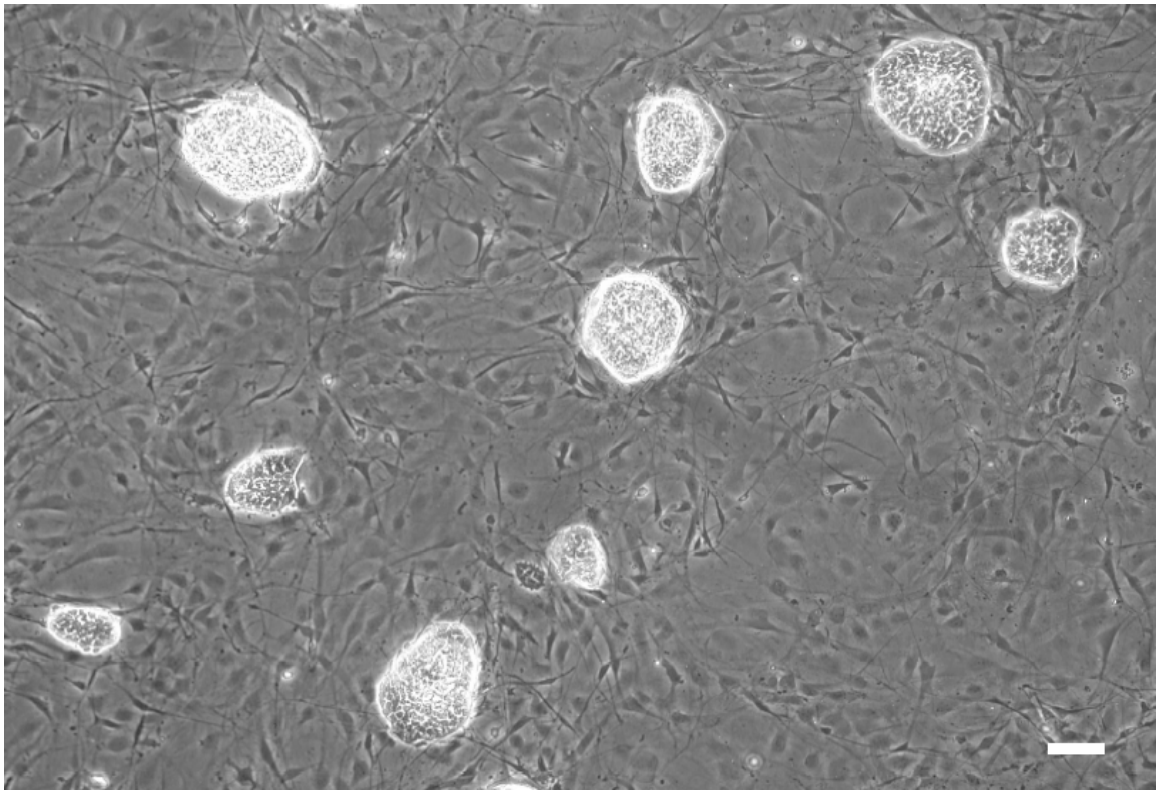

Figure 1. The undifferentiated ES cells grow of on MEFs and form colonies containing between 500-1000 undifferentiated stem cells. Scale bar = 50μm.

LIF is essential for maintaining the ES cells undifferentiated and it was recently reported (Keller, 2005) that in the presence of appropriate batches of fetal calf serum (FCS) recombinant LIF can replace the feeder cell function. However, in our hands, ES cells cultured on gelatin-coated dishes without feeder cells tended to differentiate by forming flat colonies containing epithelial-like cells. Since MEFs provide not only secreted factors (LIF included), but also extracellular matrix and cellular contacts important for the maintenance of undifferentiated stem cells state, we cultured ES cells both on MEFs and with the addition of recombinant LIF in the culture medium.

To prevent the undesired proliferation of feeder cells, we inactivated them with Mitomycin C, that inhibits DNA synthesis and replication by forming cross-links

between the complementary strands of DNA, thus preventing the separation of the complementary DNA strand.

The protocol for neuronal differentiation consists of tree steps:

1. Induction of the neuronal differentiation
2. Amplification of the neuronal precursors
3. Differentiation of ES-derived neuronal precursors

3.1.1. Induction of the neuronal differentiation

In order to induce neuronal differentiation of ES cells, stromal feeder cell line MS5 was used (kind gift of Dr. Studer). MS5 are preadipocytic mesenchymal cells that were originally developed to support *in vitro* growth and long-term expansion of highly purified haematopoietic stem cells and were subsequently described to induce neuronal differentiation of embryonic stem cells (Barberi et al, 2003).

Neural induction was initiated by plating undifferentiated ES cells on Mitomycin C-treated MS5 feeder as single-cell suspension at low density (250 cells/cm^2). ES cells seeded on this feeder layer and exposed to serum replacement medium, formed small epithelial structures (Fig. 2A) and after a few days, many cells in the structure were immunoreactive to neural precursor markers such as nestin. By day 6 (Fig. 2B), virtually all ES cell-derived colonies were positive for nestin (Fig. 2C).

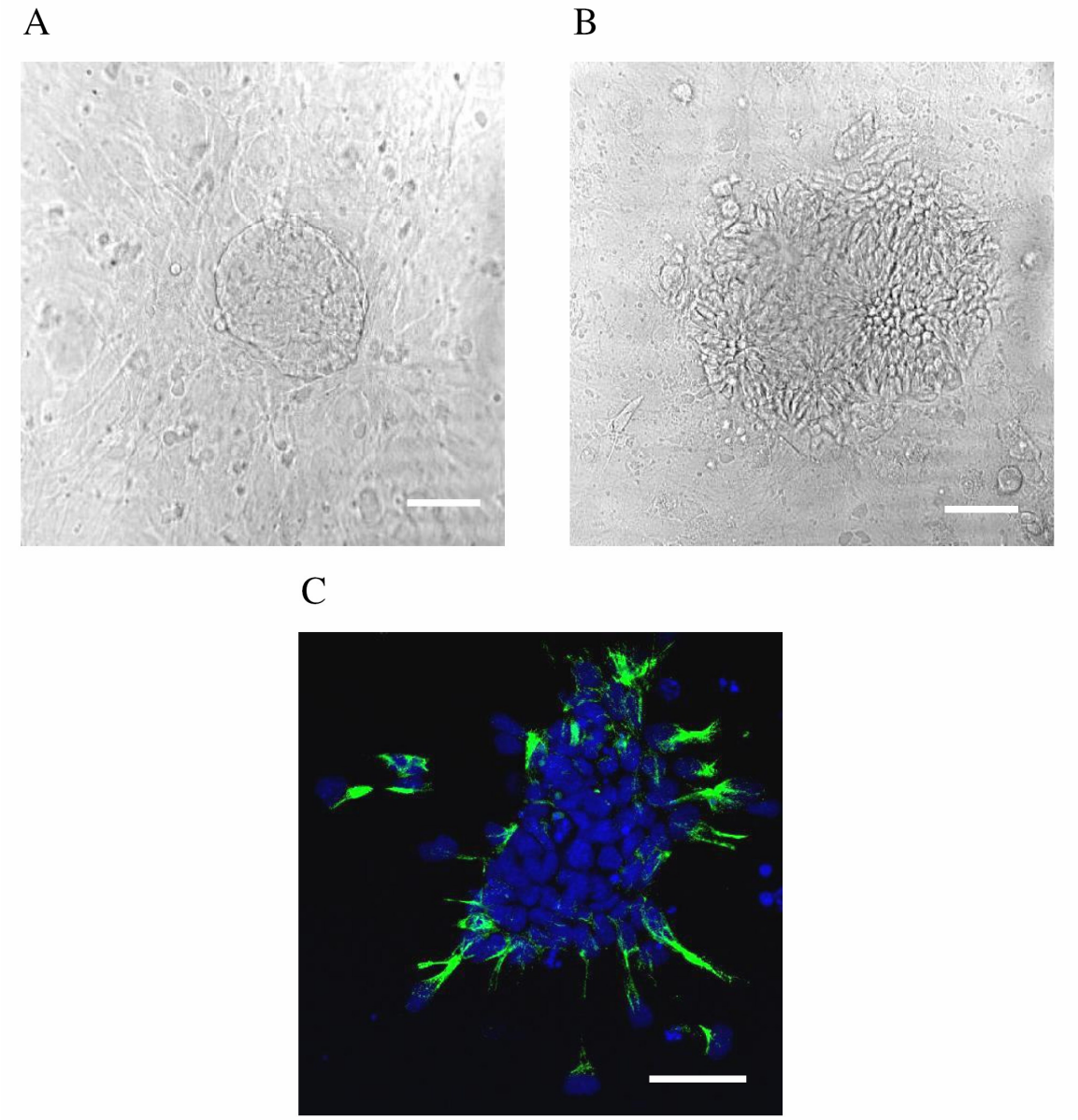

Figure 2. The growth of ES cells on MS5 feeder in serum replacement medium. DIC image of ES cells at 4 days **(A)** and 6 days **(B)** after plating. **(C)**: Nestin-positive (green) colony of ES cells on day 6. The cell nuclei were stained with Hoechst 33342 (blue). Scale bar = 50µm.

The positive staining for nestin was mainly detected on the borders of the colonies (Fig. 2C) where the cells were in better contact with stromal cells. Therefore, a further step of selection and amplification of precursors was necessary.

3.1.2. Amplification of the neuronal precursors

The second step of the protocol involves the selection and amplification of the ES-derived neuronal precursors in the presence of mitogen, basic fibroblast growth factor (bFGF). In the original protocol, this step was performed by changing the medium composition and the neuronal precursors were amplified directly on the stromal feeder cells. The presence of the feeder layer could interfere with the extracellular recordings on the MEAs where a good contact of the neurons with the electrode is required to obtain a good electrical signal. Therefore, we had to modify the original protocol to eliminate the feeder layer.

To separate the ES colonies from the MS5 feeder layer we could not use chemical digestion with trypsin because this would produce the detachment of the whole feeder layer together with the ES colonies. We chose to mechanically separate ES colonies from feeder cells by using Hank's balanced salt solution (HBSS; see Methods). HBSS is a calcium-free solution that interferes with cell-adhesion proteins, i.e. cadherins, that are calcium-dependent.

After brief incubation with HBSS, by flushing the solution through the pipette tip near the colonies, the ES colonies detached leaving the MS5 cells attached to the culture dish. The detached colonies were then transferred on polyornithine-fibronectin-coated dishes and KSR medium was added. After 2-3 hours, to allow the deposition of the cells, half of the medium was changed with N2 medium containing 10ng/ml bFGF and 1µg/ml fibronectin (amplification medium) to start the amplification/purification step.

During this step, the cells expanded from the colonies and in 2-3 days formed a monolayer of cells, almost all of which were positive for nestin (96.66% ± 0.88%; (n=3); 690 total cells analyzed) (Fig. 3).

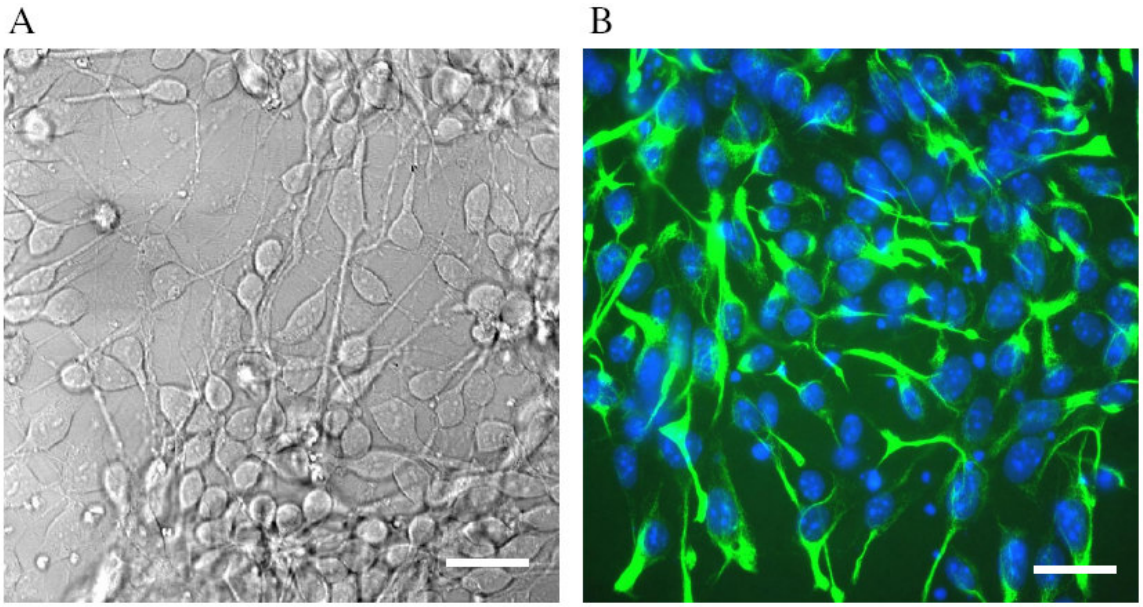

Figure 3. ES-derived neuronal precursors after 2 days of amplification. **(A)**: DIC image of precursors. **(B)**: The precursors spread forming monolayer and almost all are positive for nestin (green). The cell nuclei are stained with Hoechst 33342 (blue). Scale bar = 25μm.

The precursors were amplified in the presence of bFGF for 4 days. During the last 2 days 200ng/ml of Sonic Hedgehog (SHH) and 100ng/ml fibroblast growth factor (FGF) 8 were added as patterning factors. The addition of FGF8 resulted in an increased cell number and SHH was added in combination with FGF8 to enrich in the final yield of neurons (Barberi et al, 2003; Lee et al, 2000).

3.1.3. Differentiation of ES-derived precursors

The differentiation is induced by removal of bFGF and addition of specific neurotrophins: brain derived neurotrophic factor (BDNF) and neurotrophin (NT) 4.

We observed that the amplification step was not possible on MEAs because the colonies that detached from MS5 did not adhere properly on the dish and cells eventually died. To bypass this problem, we introduced further modification in the protocol.

Precursors were first amplified on tissue culture dishes, detached with trypsin treatment and then plated on polyornithine-FCS-laminin-coated MEAs. Trypsin was neutralized by the addition of fetal calf serum (FCS) to the N2 medium containing 10ng/ml BDNF, 10ng/ml NT4 and 1µg/ml laminin (differentiation medium). In this way, the cells attached well on the MEA dish.

The next day the medium was replaced with differentiation medium without serum and the ES-derived neurons were maintained in culture up to 10 weeks by changing half of the differentiation medium twice a week.

3.2 MATURATION OF ES-DERIVED NEURONS AND CULTURE CHARACTERIZATION

Within 1-2 days after the differentiation induction, the ES-derived precursors (Fig. 3A) started to elongate and to extend neurites. After 1 week of differentiation, cells assumed a typical neuronal morphology and generated extensive network of processes (Fig. 4A).

ES-derived neurons expressed the post-mitotic neuronal marker β–tubulin III starting from 3 days after differentiation induction (Fig. 4B). A microtubule associated protein (MAP) 2 was also used to mark ES-derived neurons, in particular the cell bodies and dendrites (Fig. 4C). These markers were present throughout the observation period.

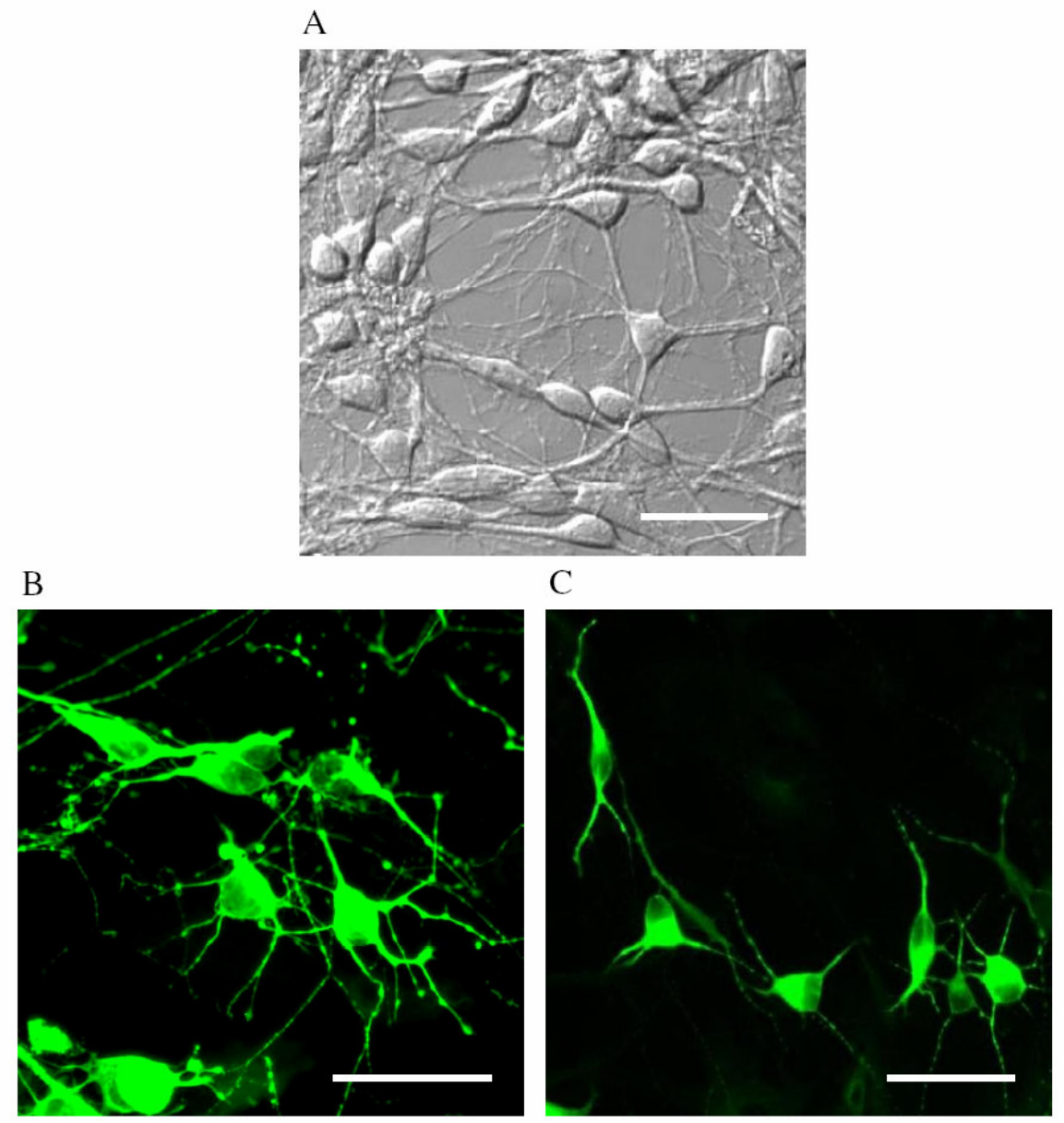

Figure 4. (A): DIC image of neurons at 7 days of differentiation. Immunofluorescence labeling of neurons at 3 days of differentiation with TUJ1 **(B)** and MAP2 **(C)** antibody. Scale bar = 25µm.

In general, the neuronal markers TUJ1 and MAP2 were coexpressed during the time course of differentiation. However, MAP2 expression was not present in all neurons during the first week of differentiation since we observed MAP2-negative/GABA-positive cells (Fig. 5) while TUJ1-negative/GABA-positive cells were never found.

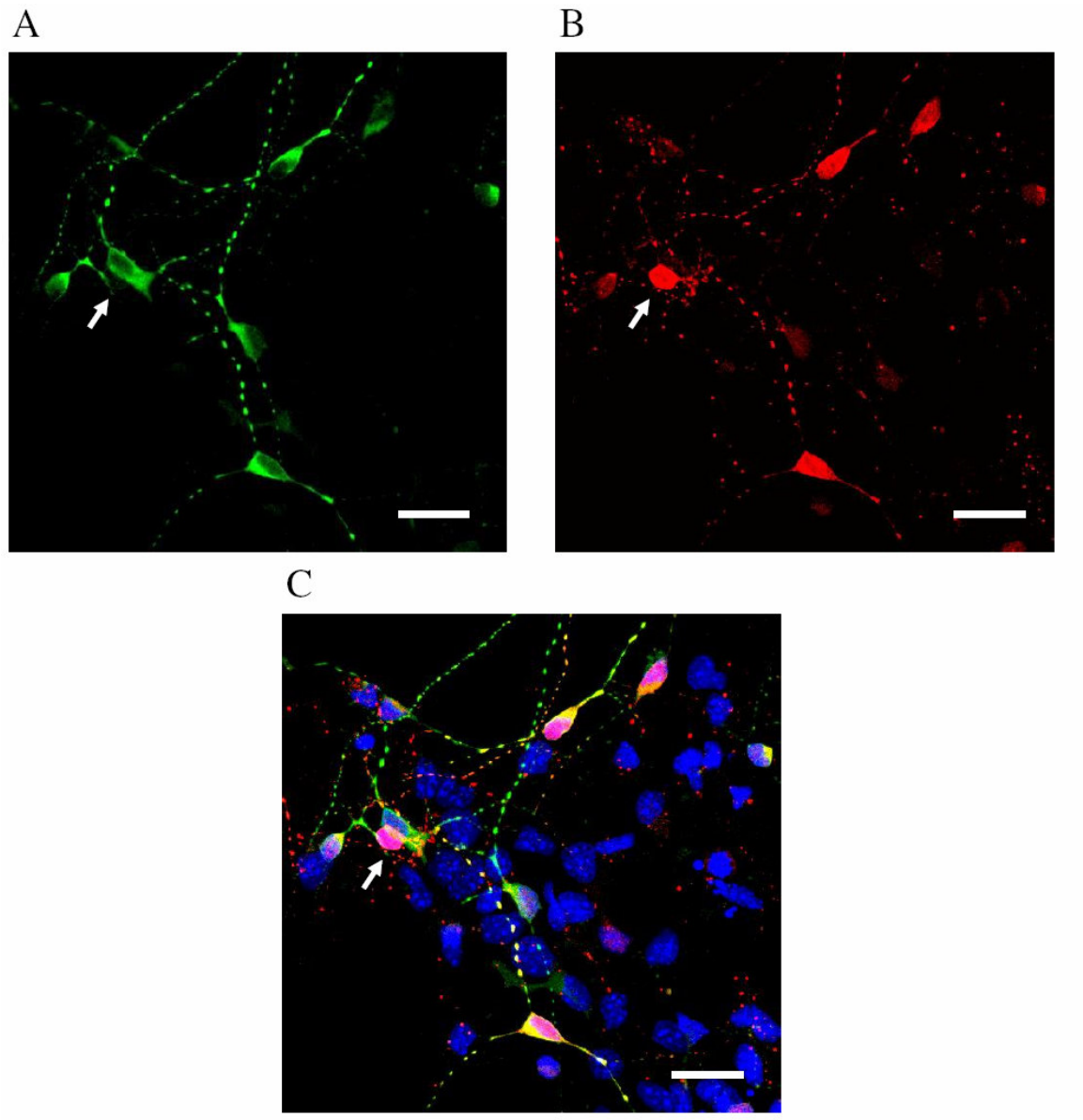

Figure 5. ES-derived neurons at 7 days of differentiation stained with anti-MAP2 **(A)** and anti-GABA **(B)** antibody. **(C):** Merged image for MAP2 (green), GABA (red) and cell nuclei stained with Hoechst 33342 (blue). White arrows indicate MAP2-negative/GABA-positive neuron. Scale bar = 25µm.

TUJ1 and MAP2 showed different intensity of expression: during the first week of differentiation, TUJ1 staining in most neurons was stronger with respect to MAP2 (Fig. 6A). At two weeks of differentiation, there was almost equal intensity of staining (Fig. 6B). At three weeks of differentiation most neurons showed stronger MAP2 staining in respect to TUJ1 (Fig. 6C). These observations are in agreement with previous findings that MAP2 is expressed in more mature neurons and that *in vivo*, the level of expression of β−tubulin III decreases during postnatal development (Jiang and Oblinger, 1992).

Figure 6. Merged images of TUJ1 (red) and MAP2 (green) staining of ES-derived neurons during the first **(A)**, second **(B)** and third **(C)** week of differentiation. Neurons stained strongly for TUJ1 during the early phase of differentiation whereas after 3 weeks of differentiation, the staining for MAP2 was stronger. Scale bar = 25 μm.

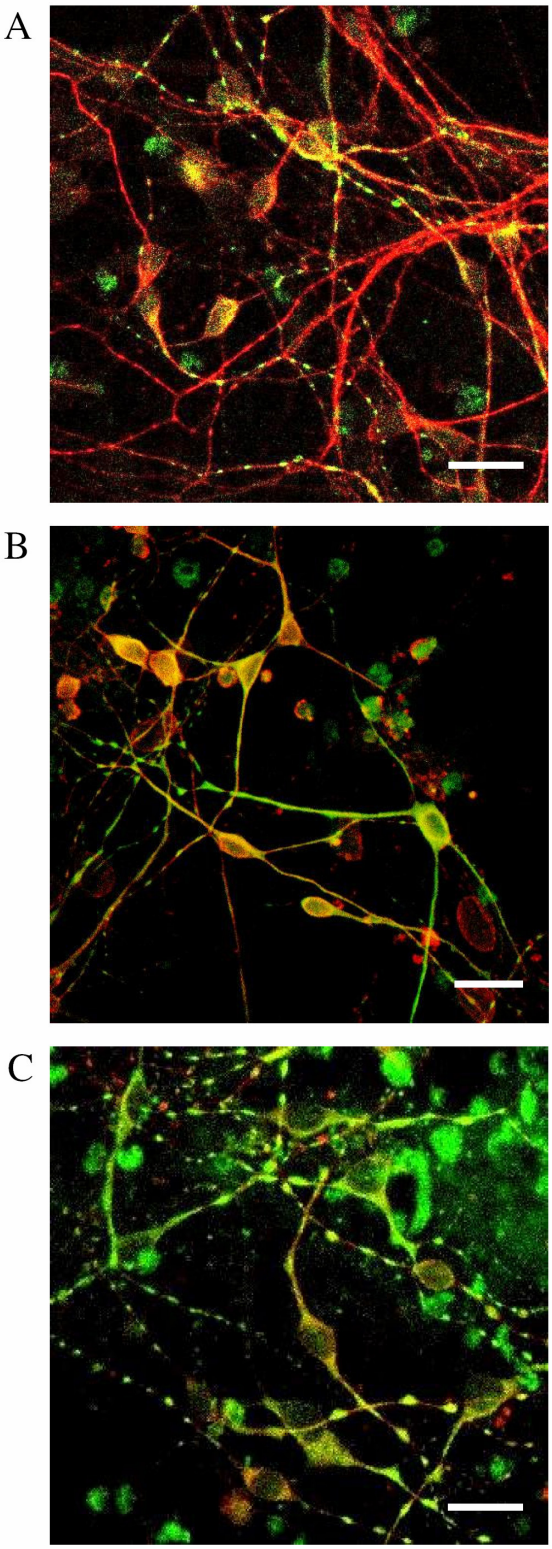
A
B
C

Of these post-mitotic neurons, at one week of differentiation almost 40% were GABAergic (Tab. 1 and Fig. 7A), less than 5% were dopaminergic (positive for tyrosine hydroxilase (TH); Tab. 1 and Fig. 7B) and less than 2% were serotonergic (positive for 5-HT; Tab. 1 and Fig. 7C). By using ChAT antibody, no cholinergic neurons were found. We suppose that all the remaining neurons were glutamatergic. However, we were not able to find the appropriate marker for glutamatergic neurons. We tested both the antibodies against glutamate and vesicular glutamate transporter 2 (VGLUT2) but we did not obtain the specific staining. CaMKII antibody stained properly the glutamatergic neurons (Fig. 7D). However, the double staining of CaMKII with TUJ did not allow an easy identification of those cells that are positive for both antibodies.

Table 1. Percentage of different neuronal subtypes at one week of differentiation.

Neuronal subtype	TUJ1-positive cells analyzed	% subtype-specific neurons*	number of experiments performed
GABAergic	2391	39.28 ± 1.86	4
Dopaminergic	578	4.89 ± 0.26	3
Serotonergic	920	1.73 ± 0.89	3

*Data values are presented as the means +/- SD.

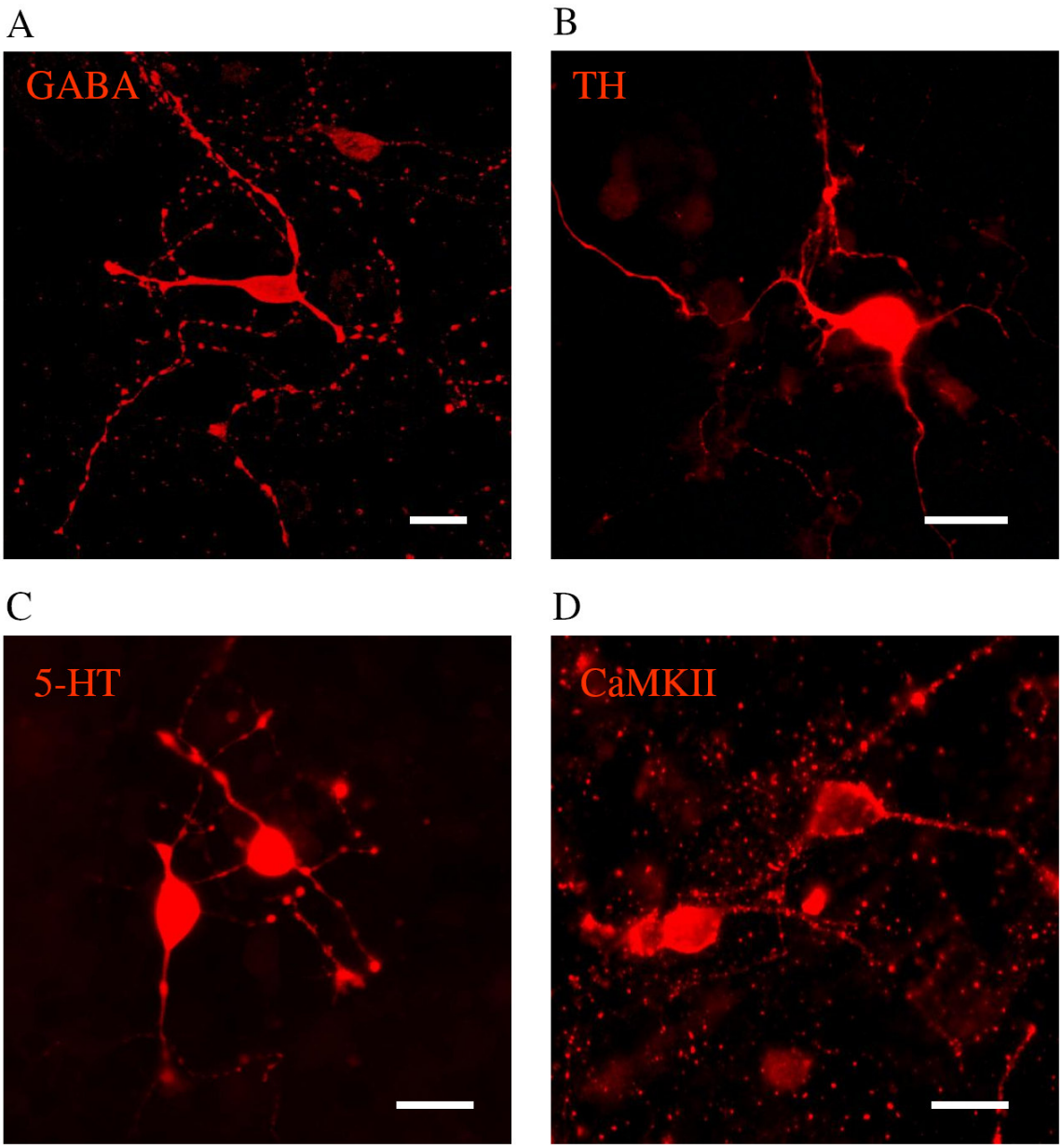

Figure 7. Neuronal subtype characterization of the culture. **(A):** GABAergic, **(B):** TH-positive dopaminergic, **(C):** 5-HT-positive serotonergic and **(D):** CaMKII-positive glutamatergic neurons. Scale bar = 15µm.

To monitor the survival of ES-derived neurons, the yield of TUJ1-positive cells was counted at 7, 10, 14 and 21 days of differentiation. Table 2 summarizes the results of at least three independent experiments for each time interval.

The percentage of neurons slightly decreased during the differentiation: from about 38% at first week of differentiation to 28% of the total cells present in the culture at three weeks of differentiation. The decrease in neuronal viability with time is in agreement with other observations (Fraichard et al, 1995).

Table 2. Percentage of neurons during the differentiation.

Days of differentiation	Total cells analyzed	% TUJ1/total cells*	number of experiments performed
7	925	37.42 ± 2.74	3
10	3214	34.12 ± 3.63	4
14	2891	30.99 ± 3.55	4
21	1516	28.37 ± 4.55	3

* Data values are presented as the means +/- SD.

Since *in vitro* differentiation can give rise to neurons, astrocytes and oligodendrocytes, we analyzed also the induction of glial cells during a period of time. ES-derived astrocytes were marked with glial acidic fibrillary protein (GFAP; Fig. 8). Very few astrocytes were observed during the first week (Tab. 3). However, already after 10 days of differentiation, more than 30% of the cells were positive to GFAP and their percentage progressively increased reaching about 50% of the population at 3 weeks of differentiation (Tab. 3 and Fig. 8). Increased numbers of GFAP-positive cells over the

observation period is in agreement with *in vivo* developmental progression and with adult neuronal stem cell differentiation studies *in vitro* (Sauvageot and Stiles, 2002; Sun et al, 2003).

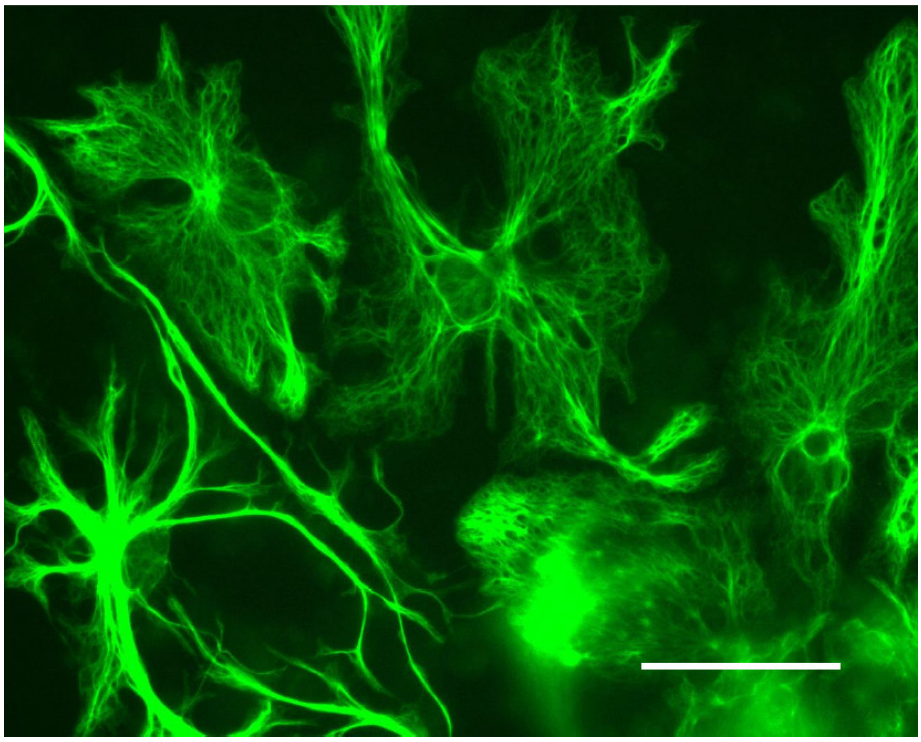

Figure 8. ES-derived GFAP-positive astrocytes at three weeks of differentiation. Scale bar = 25 µm.

Table 3. The percentage of astrocytes during the differentiation.

Days of differentiation	Total cells analyzed	% GFAP/total cells*	number of experiments performed
7	615	8.74 ± 3.57	3
10	1786	32.54 ± 4.00	3
14	644	33.62 ± 12.49	3
21	845	46.48 ± 1.46	3

* Data values are presented as the means +/- SD.

By using either O4 or SMI-94 antibodies, we did not detect any oligodendrocytes in our culture.

As the differentiation proceeded, the ES-derived neurons assumed a mature morphology (Fig. 9), connected to each other and grew in close contact with glial cells. At 3 weeks of differentiation, neurons and glial cells represented almost 80% of the total cell number (Tab. 2 and 3). The presence of non-neuronal cells (about 20% of total cells) was in part a consequence of the use of FCS during the first few days of differentiation.

To block the overgrowth of non-neuronal cells, we treated our culture with proliferation blockers Mitomycin C or cytosine-β-D-arabinofuranoside (Ara-C) but these agents resulted toxic for ES-derived cultures causing increased cell death and detachment from the MEA dishes. To avoid the use of serum, we also tried the mechanical dissociation in HBSS solution that does not require neutralization with FCS before

plating on MEA. This modification of the protocol resulted in a decreased maturation of glial cells which affected negatively adhesion and long-term survival of the neurons. This was not surprising since it is known that glial cells secrete survival factors for the neurons, and also form an adhesive substratum for the neuronal cells *in vitro* (O'Shea, 1999).

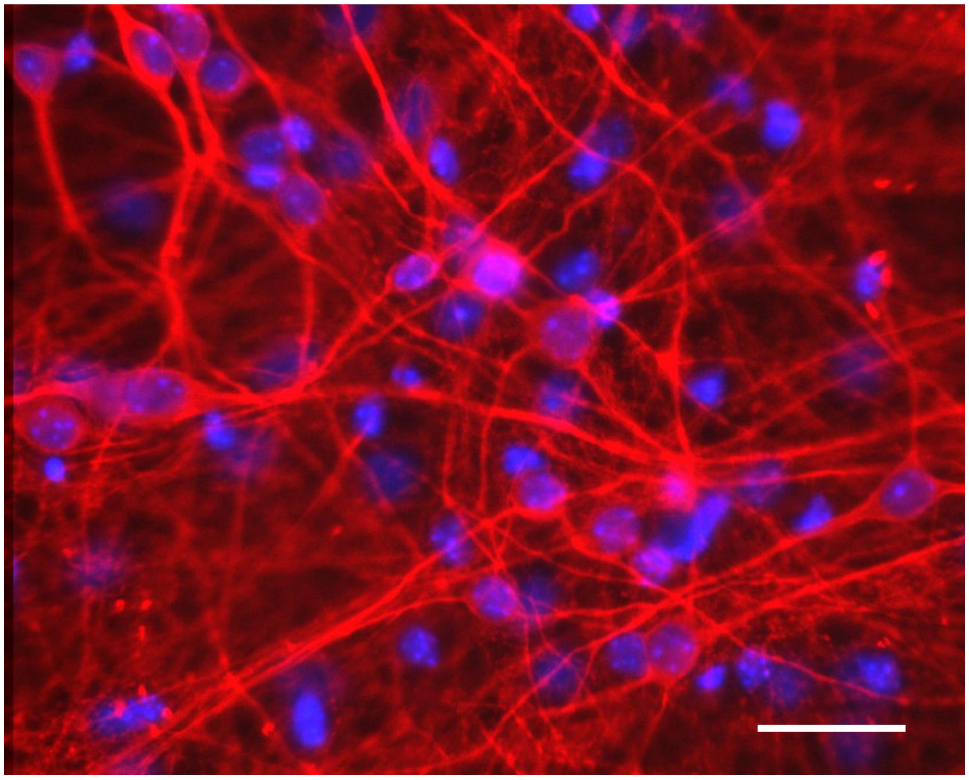

Figure 9. ES-derived TUJ-positive neurons (red) at 3 weeks of differentiation. The cell nuclei are stained with Hoechst 33342 (blue). Scale bar = 25µm.

3.3 INTRACELLULAR RECORDINGS

To confirm that differentiation of ES cells produced functional neurons, intracellular recordings with patch pipettes were performed at 7, 14, 21 and 28 days after differentiation induction (41 cells). The resting membrane potential was – 43 ± 4 mV after one week (n=8) and increased to – 68 ± 7.8 mV after 3 weeks (n=13). The input resistance was 2 ± 1.3 GΩ during the first week and decreased subsequently to 1.4 ± 0.6 GΩ in the ES-derived neurons.

After one week, a depolarizing current pulse evoked at most one AP with mean amplitude of 12.9 ± 5 mV s.d. (n=8). After 2 weeks of differentiation ES-derived neurons produced APs with amplitude of about 50mV, but a tonic discharge of APs was evoked only in 1 out of 8 cells analyzed. After 3 weeks, 4 out of 12 cells fired trains of APs and after 4 weeks, 9 out of 13 cells discharged APs in a sustained way, but neurons with a transient firing were still observed.

Examples of current-clamp recordings of ES derived neurons at 7, 14, 21 and 28 days of differentiation are shown in Figure 10. After 4 weeks of differentiation, in some cells a depolarizing current pulse did not evoke APs and voltage clamp recordings from these cells indicated the presence of voltage gated K^+ currents but not of Na^+ current (not shown). As the percentage of glial cells in the culture increased with time, these recordings were presumably obtained from glial cells.

These results demonstrated that at single-cell level, functional ES-derived neurons were obtained.

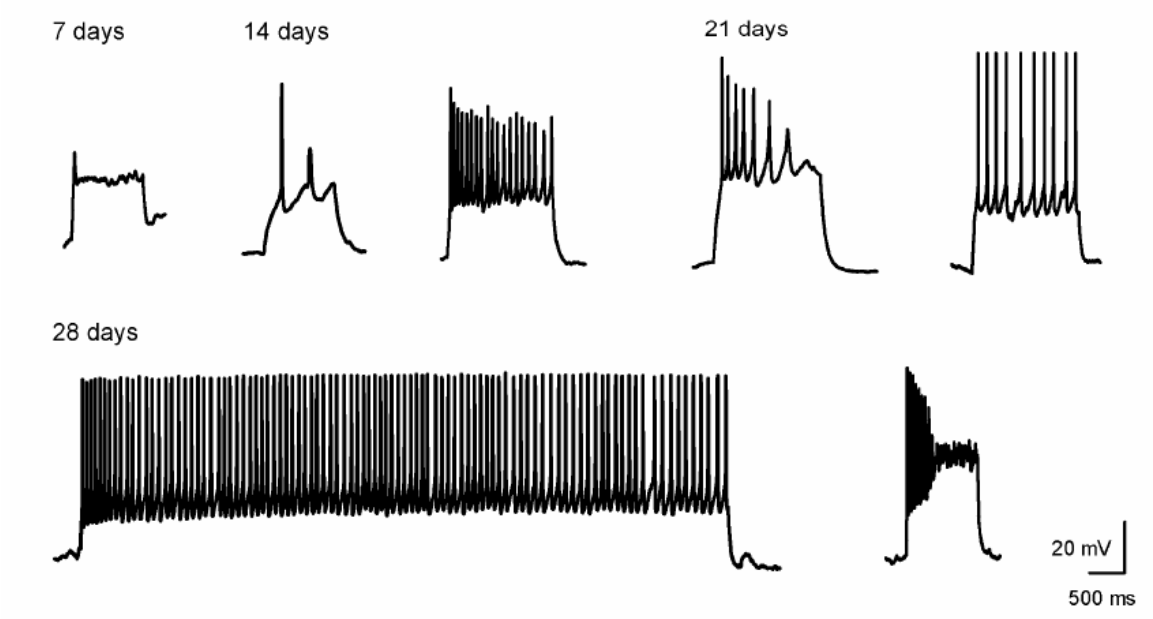

Figure 10. Electrophysiological characterization of APs firing of ES-derived neurons. ES-derived neurons at different days of differentiation (7, 14, 21, 28) were recorded in whole cell current clamp mode at rest, i.e. with no bias current injected. **7 days**: step of 20 pA of 1 s duration. **14 days**: (first trace) step of 10 pA of 1 s duration; (second trace): step of 12 pA of 1.5 s duration. **21 days**: (first trace): step of 15 pA of 1.5 s duration; (second trace): step of 35 pA of 1.5 s duration. **28 days**: (first trace) step of 20 pA of 9 s duration. (second trace): step of 30 pA of 1 s duration.

3.4 ELECTRICAL RECORDINGS ON MEAs

Multi-electrode array (MEA) is a non-invasive technique that allows to record extracellular electrical activity from 60 electrodes, spaced only a few hundred microns apart, and all incorporated into a single chip.

In order to test the appearance of spontaneous activity in ES-derived neuronal cultures, neuronal precursors were plated and induced to differentiate directly on the MEA.

After one week of differentiation of ES-derived neurons on the MEA, it was possible to record the extracellular voltage signals that corresponded to action potentials (APs) having a shape very similar to that observed in cultures obtained from neonatal hippocampal rat neurons (Fig. 11). However, in general, ES-derived neurons had a greater proportion of small spike amplitudes than hippocampal neurons. In fact, less than 5% had amplitude higher than 50μV although amplitudes large as 100μV could be observed. In the hippocampus, the percentage of spikes with amplitude higher that 50μV was more than double and spikes could reach 200μV.

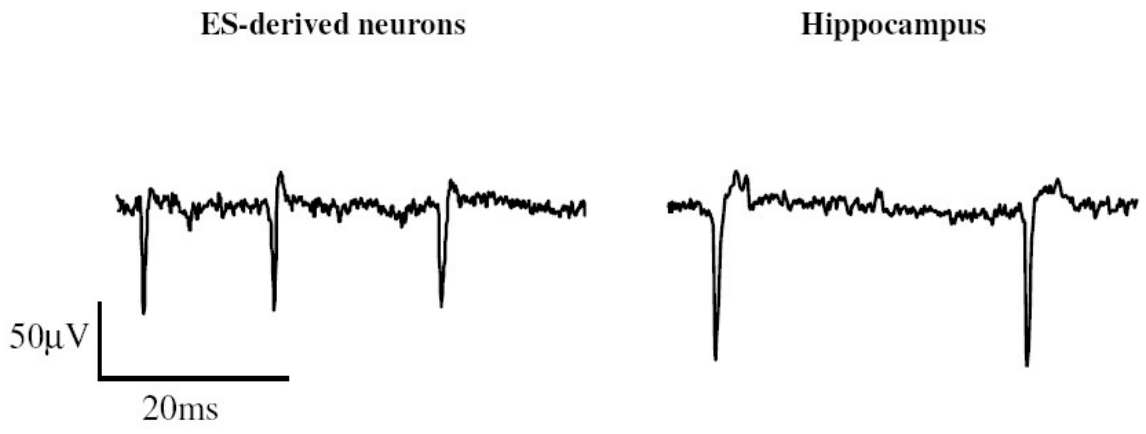

Figure 11. Example APs spontaneously recorded from the single electrode of the MEA from ES-derived and hippocampal neurons respectively.

Extracellularly recorded APs varied in number of active sites and amplitude of spikes for different electrodes and in different cultures because they depend on the quality of the contact of the cells with the electrodes. Despite these differences, we observed an increase in the number of active sites (electrodes recording spontaneous activity) with the progression of ES-derived neurons differentiation. In fact, during the first week of differentiation on MEAs, we recorded APs from few (less than 5) electrodes of the MEA. During the second week new active sites were observed (from 5-10) and on the third week of differentiation we were able to record the APs from up to 20 electrodes and the spike amplitudes were higher.

These results demonstrated that ES-derived cells differentiate into functional neurons. Since the protocol modifications allowed us to maintain these cells in culture for long periods (up to 10 weeks) the formation of neuronal networks could be foreseen. To investigate whether these cells are able to form a network and to study some of the network properties of the ES-derived culture, we used a primary culture of dissociated hippocampal neurons previously investigated in our lab (Bonifazi et al, 2005; Ruaro et al, 2005) for comparison.

A hippocampal culture was prepared from three-day-old Wistar rats. Briefly, dissociated hippocampal neurons were plated on polyornithine-matrigel-coated MEAs and maintained in a medium containing 5% FCS and Ara C to block glial proliferation (for the exact composition see methods). The hippocampal culture was mainly composed of neurons (positive to TUJ1; Fig. 11A), while the percentage of glial cells was around 10% (Fig. 11B). Approximately 10% of the neurons were GABAergic (Fig. 11C) and

about 90% were glutamatergic (positive to vesicular glutamate transporter 2 (VGLUT2); Fig. 11D); no serotonin or dopaminergic neurons were detected (Bonifazi et al, 2005).

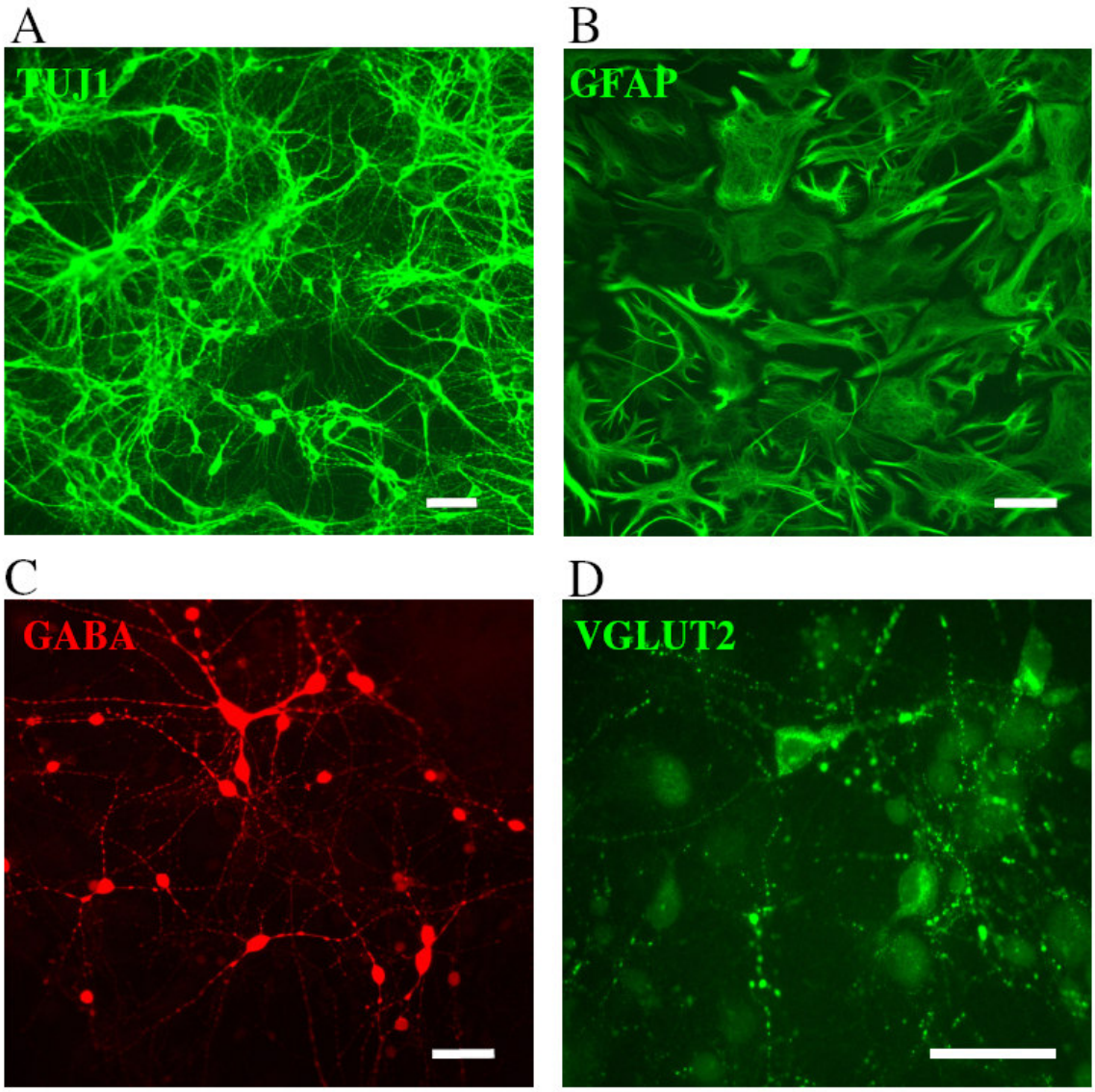

Figure 12. Cellular composition of hippocampal cultures at 3 weeks of differentiation. Immunofluorescence staining of: **(A):** neurons (TUJ1–positive), **(B):** glial cells (GFAP positive), **(C):** GABAergic neurons (GABA positive), **(D):** glutamatergic neurons (VGLUT2 positive). Scale bar = 50 µm.

By performing a double immunofluorescence staining of neurons (TUJ1-positive) and glia (GFAP-positive) for both cultures, we observed that the morphological appearance of ES-derived and of hippocampal cultures was very similar (Fig. 13).

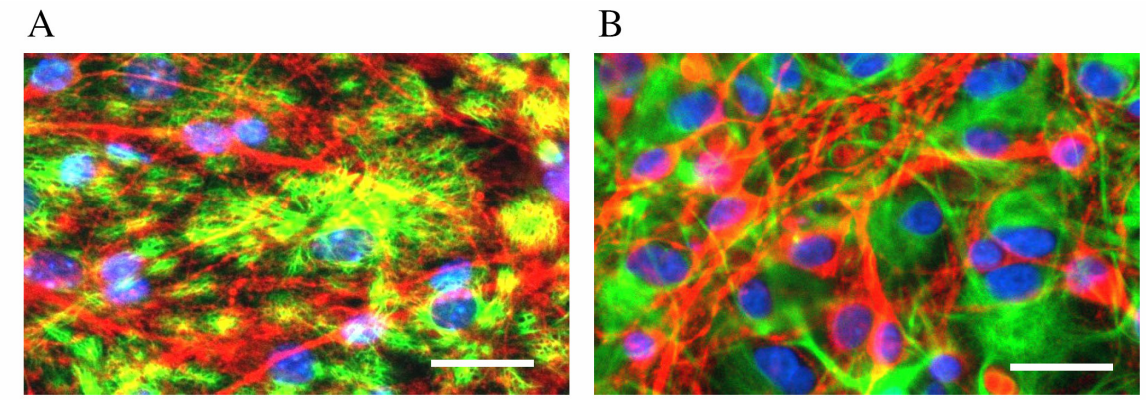

Figure 13. Immunofluorescence staining of ES-derived **(A)** and hippocampal **(B)** culture at 3 weeks of differentiation. Scale bar = 25µm.

3.5 SPONTANEOUS ACTIVITY OF MATURING ES-DERIVED NETWORKS

Spontaneous activity is a common characteristic of developing neuronal networks both *in vivo* and *in vitro*, which is believed to play an important role in network development (Demas et al, 2003; Lahtinen et al, 2002; Leinekugel et al, 2002; Lestienne 2001; Limpert et al, 2001; Van Pelt et al, 2004 and 2005). In order to evaluate the distribution and propagation of the spontaneous activity in ES-derived neuronal cultures, ES-derived neuronal precursors were plated on MEA and induced to differentiate. After 3 weeks, spontaneous activity was recorded and compared with that of dissociated hippocampal neuronal cultures.

Figure 14 illustrates the spontaneous activity of ES-derived networks (panels A and B) and of hippocampal networks (panels C and D). Simultaneous extracellular recordings are shown in A and C for ES-derived and hippocampal networks respectively.

APs were detected on different electrodes, and bursts of APs recorded simultaneously from several electrodes invading the entire network were often observed. The global electrical activity of the network was described by computing the firing rate of the entire network FR (t) (see Methods) counting the total number of recorded APs in a given bin width. As shown in the upper panels of Figure 14B and D, the FR (t) of both ES-derived and hippocampal networks had large peaks corresponding to the simultaneous firing of several neurons, separated by periods where only occasional APs were observed. The global electrical activity of the network can also be visualized by considering raster plots – where a dot represents the occurrence of an AP - of several electrodes. Raster plots from ES-derived and hippocampal networks are shown on the bottom panel of Figure 14B and D respectively. In raster plots a vertical black line indicates that APs were recorded simultaneous from all – or most of – extracellular electrodes of the MEA.

Figure 14. Multielectrode recording of spontaneous activity of ES-derived network at 25 days of differentiation. **(A):** Snapshot of 1 second of spontaneous activity at selected electrodes of the multielectrode array (MEA) during a burst. **(B):** Temporal analysis of 2 minutes of spontaneous activity. Upper panel: 2 minutes of global activity of the network; firing rate (number of action potentials (APs) in a bin width of 250 ms) recorded by all electrodes of the MEA. Lower panel: spontaneous activity recorded by each single electrode in time bins of 250 ms; the intensity of the activity at the electrode in a particular time bin is represented in greyscale (see Materials and Methods). **(C)** and **(D)** represent the same analyses as in **(A)** and **(B)** for a hippocampal network after 3 weeks in culture.

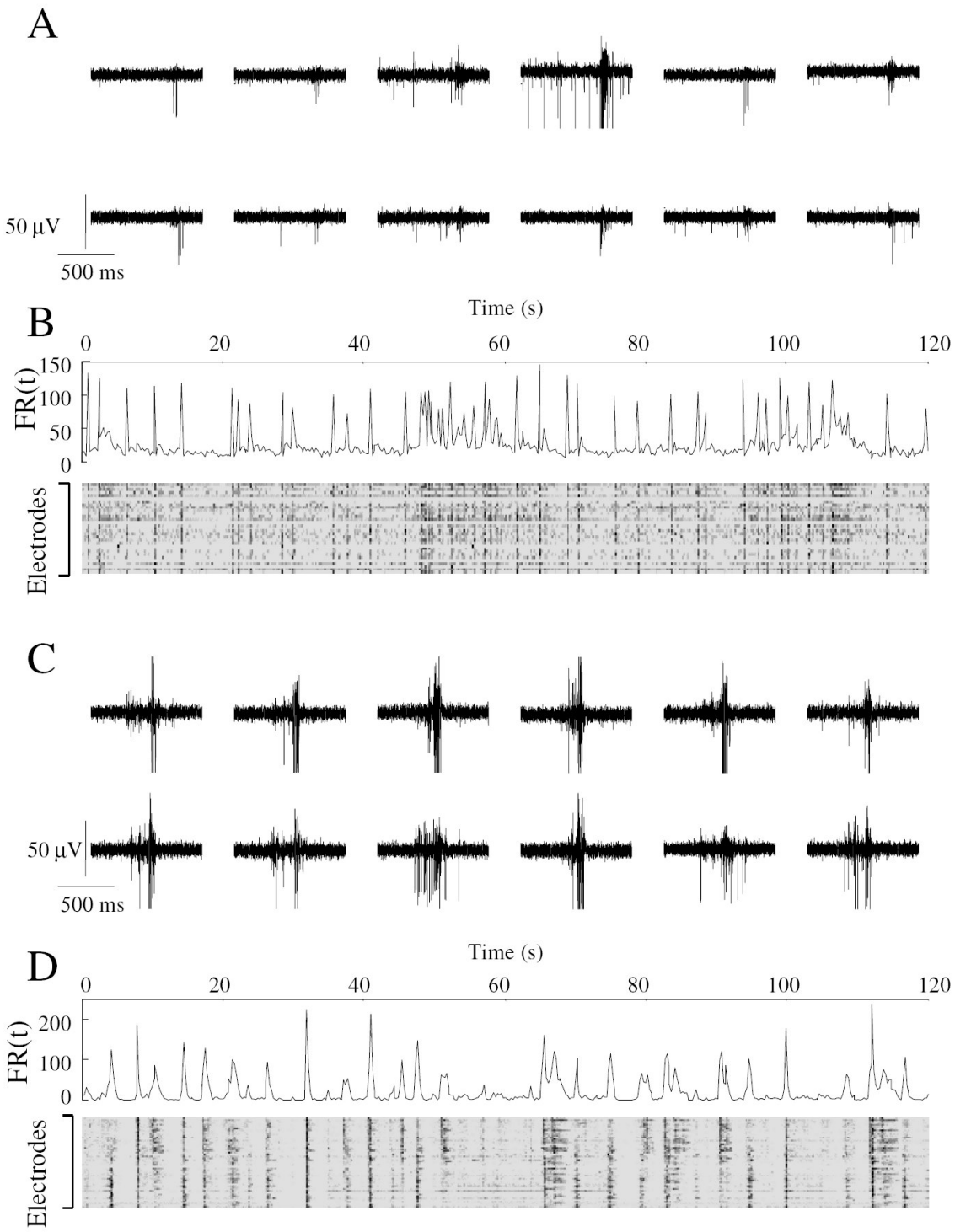
A
50 µV
500 ms
B
Time (s)
0
20
40
60
80
100
120
FR(t)
150
100
50
0
Electrodes
C
50 µV
500 ms
D
Time (s)
0
20
40
60
80
100
120
FR(t)
200
100
0
Electrodes

A comparison between the FR (t) and raster plots from ES-derived and hippocampal networks shows that in both networks large bursts of simultaneous activity were observed. The size of these bursts was random and did not have any regular structure. These bursts did not have any obvious periodicity and their occurrence could not be predicted. We observed spontaneous activity in these cultures (n=5) for more than two months and, in one case, up to three months. Although the firing pattern of both types of networks was quite similar, the spontaneous activity baseline was slightly higher in ES-derived networks than in hippocampal networks (compare upper panels of Fig. 14B and D). This was likely due to the presence of a tonic firing of small amplitude, resulting in rare periods of quiescent activity (compare bottom panels of Fig. 14B and D). This tonic firing of small amplitudes spikes (see Fig. 14A) was reminiscent to that of immature hippocampal networks (data not shown).

To further investigate the firing pattern of both networks, the firing rate was binned and the probability distribution of the number of spikes and active electrodes present in each bin was computed (see Methods). Both networks had a probability distribution of the number of spikes per bin fitted by lognormal distributions (Fig. 15A and B), indicating the presence of multiplicative effects (Limpert et al, 2001) among the firing pattern of individual electrodes, broadening the range over which large amount of spikes per bin can be observed.

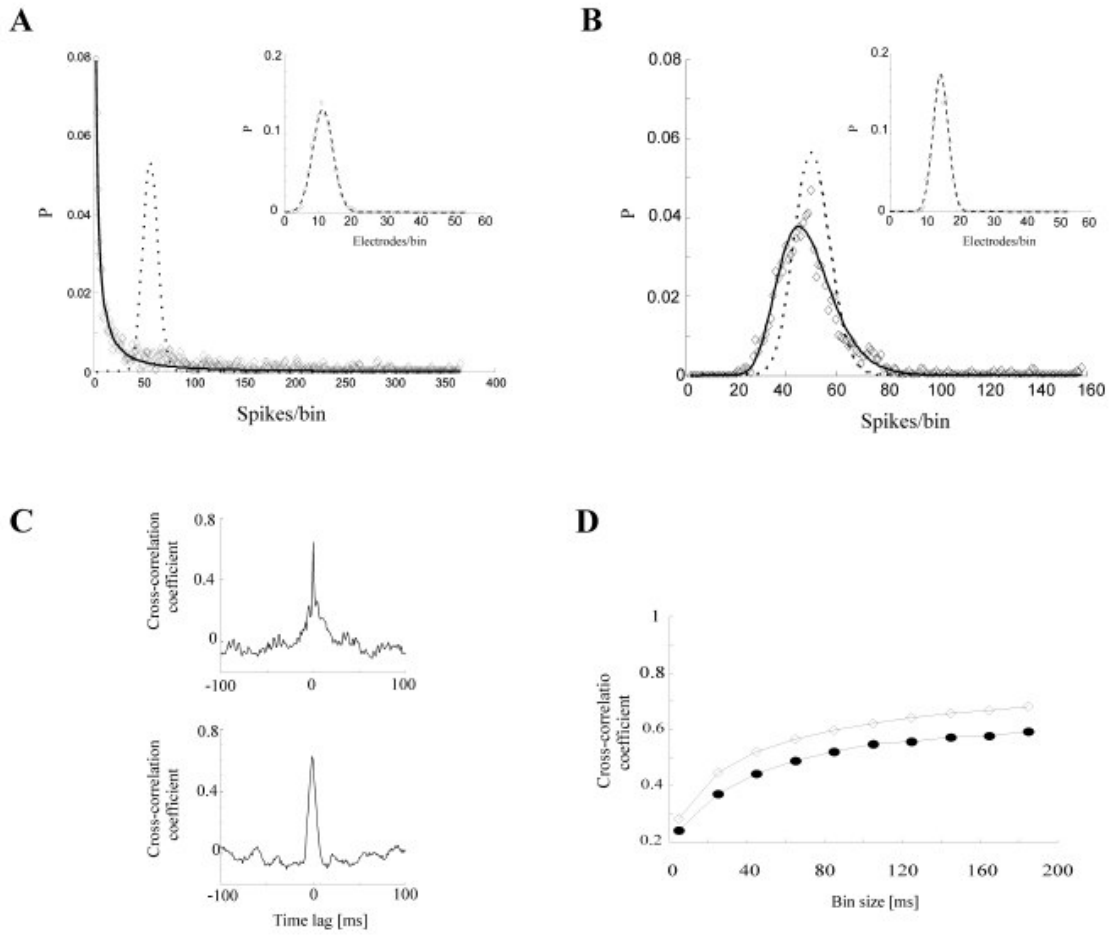

Figure 15. Correlated firing. **(A, B):** Probability distribution of the number of spikes per bin (250 ms) in the hippocampal- and ES-derived networks, respectively. Both networks are fitted by a lognormal distribution (solid line) and not by a Poissonian distribution (dashed line), as expected in the case of random firing among neurons. The skewed lognormal distribution and its long right tail account for the presence of few large bursts, containing several hundreds of spikes, and occurring in both networks. Insets: probability distribution of the number of active electrodes per bin. The dashed line represents a Poissonian fit, indicating that the pattern of active electrodes in each time bin occurs at random. **(C):** Examples of cross correlation between couple of electrodes 1 mm apart, in the hippocampal- (top panel) and ES-derived networks (bottom panel). **(D):** Dependency of the network cross correlation on the bin size used for both ES-derived networks (filled circle) and hippocampal networks (open diamond).

The lognormal fit, characterized by a long right tail, also excluded a random firing pattern typically described by poissonian distributions (Dayan and Abbott, 2001). Moreover, the presence of tonic firing in ES-derived networks was further revealed by the presence of a peak in the lognormal distribution, centered on the number of active

electrodes. This means that at least one spike was present in each bin most of the time in contrast to hippocampal networks, where small numbers of spikes fired in each time bin have the highest probability.

Although the network firing pattern was not random and was dependent of multiplicative interactions among neurons, the number of active electrode in each bin followed a poissonian distribution (Fig. 15A and B insets), suggesting that the pattern of active electrode in during each time bin occurred at random.

In both networks types, cooperative effects between neurons recorded at distant electrodes were also indicated by their high cross-correlation coefficient (Fig. 15C).

The degree of connectivity within the network was quantified by computing the network correlation, defined as the average cross-correlation $< \rho >$ among electrical recordings from active electrodes, i.e. exhibiting evident APs (see Methods). As shown in Figure 15D, $< \rho >$ increased with the size of the bin width, i.e. the size of the time window over which correlations were considered. For small values of the bin width, i.e. less than 20 ms, the value of $< \rho >$ was lower than 0.1 indicating that spontaneously occurring APs were almost completely uncorrelated on a short time scale. At larger bin width (around 200 ms), as there is an increasing number of observations per bin there is an increasing probability of observing correlations and the value of $< \rho >$ increased to about 0.5 in both networks. This observation indicates a larger correlation of spontaneously occurring APs on a longer time scale. The dependence of $< \rho >$ on the used bin width is a consequence of the biophysical mechanisms underlying synaptic transmission and the generation of APs (Bonifazi et al, 2005): synaptic release and AP

initiation in different neurons is statistically independent at the ms level, but becomes correlated in the presence of a common input lasting some hundreds of ms.

3.6 SPREAD OF THE EVOKED ELECTRICAL ACTIVITY IN THE NETWORK

The propagation of electrical excitation in a network is a proof of the presence of chemical and electrical synaptic pathways and of functional network formation as has been previously shown in different studies on hippocampal (Ruaro et al, 2005) and cortical networks (Corner, 1994; Canepari et al, 1997; Marom and Shahaf, 2002).

Therefore the spread of the evoked activity was studied in ES-derived networks cells cultured on MEA. Electrical activity was evoked by delivering brief voltage pulses to the extracellular electrodes of the MEA (see Methods). These voltage pulses induced a transient depolarization of neurons in good electrical contact with the stimulating electrode possibly triggering the initiation of an AP. When a bar of electrodes was stimulated (black squares in the grid of Fig. 16), APs were evoked in neurons on nearby electrodes with a latency of some ms. These evoked APs propagated over almost the entire network with a progressively longer delay (Fig. 16A).

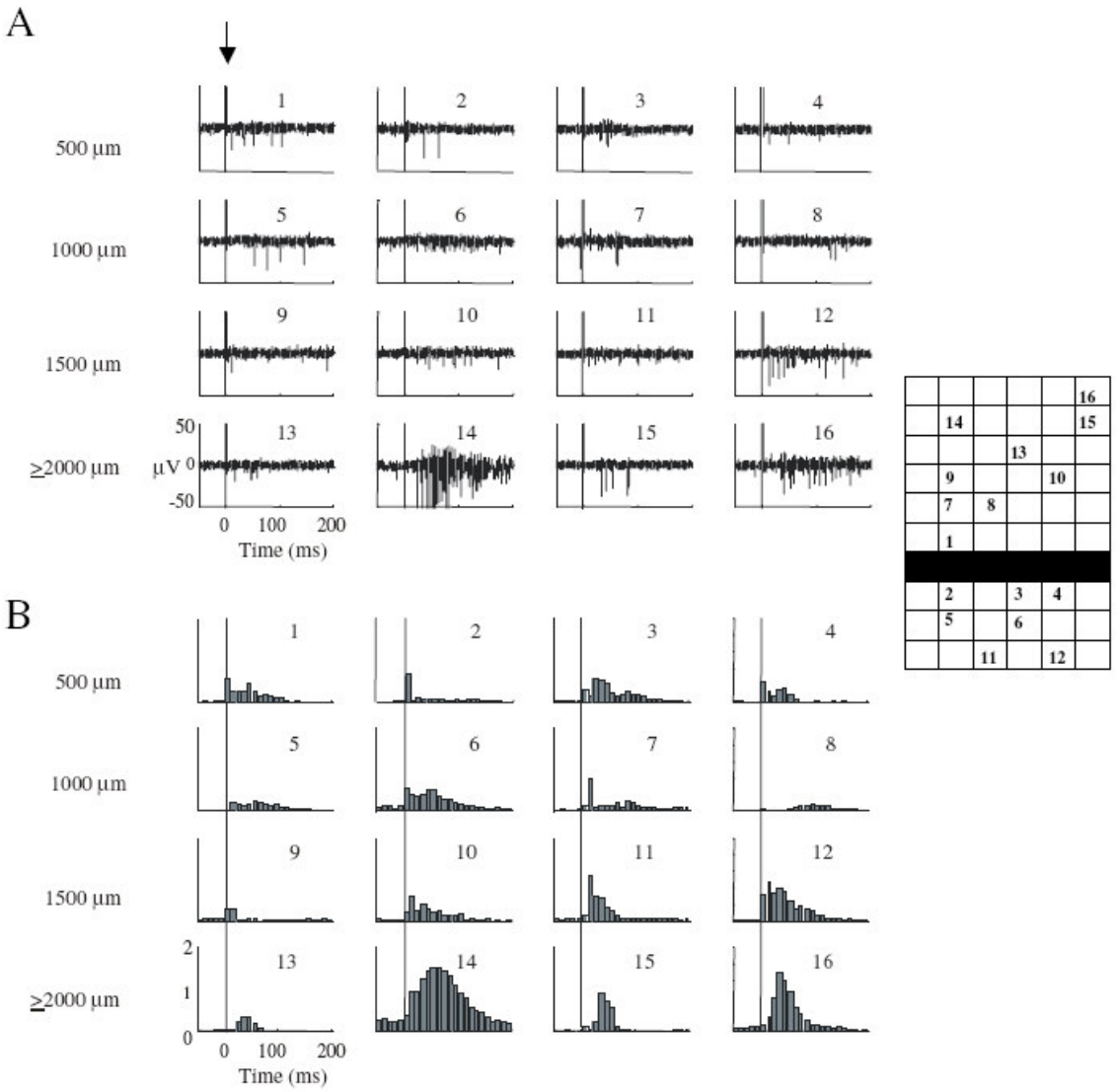

Figure 16. Evoked electrical activity in embryonic stem cell (ES)-derived networks. **(A):** Examples of extracellular voltage recordings after the stimulation of a bar of electrodes (black line in the scheme on the right) with a bipolar voltage pulse of 900 mV. **(B):** Peristimulus time histogram (PSTH) of the evoked activity from 16 electrodes of the multielectrode array (MEA). The thin vertical line indicates the stimulation artifact. Data averaged over 100 repetitions of the same stimulation.

The latency of the first evoked AP at electrodes near the stimulating bar, as the one indicated by the # 1 was less than 10 ms. Clear burst of evoked APs at electrodes distant more than 3 mm from the stimulating electrodes, as electrodes # 14,15 and 16 were observed. The latency of the first evoked APs at these more distant electrodes was

around 40 ms. The results shown here are very similar to those previously described for hippocampal cultures (Bonifazi et al, 2005; Ruaro et al, 2005) and for cortical cultures (Jimbo et al, 1999 and 2000; Potter, 2000).

The variability of the evoked electrical response was characterized by computing the peristimulus time histograms (PSTHs), obtained by averaging evoked response over 100 repetitions of the same stimulus (Fig. 16B). The peak of the PSTH of the activity recorded on more distant electrodes occurred at progressively longer times: at a distance of about 2000 μm from the stimulating electrodes, the peak amplitude of the PSTH occurred with a delay of about 40 ms from the stimulus. The evoked response was usually composed of a first reproducible AP, occurring with a similar timing in every trial, followed by less reproducible APs (Fig. 16B) as previously described for cortical networks (Jimbo et al, 2000). The standard deviation of the latency of the first evoked AP, usually referred to as its "jitter", was used to measure the reproducibility of the evoked AP. A significant correlation between jitter and latency of the first evoked AP was observed in ES-derived networks ($\rho = 0.63$, $n = 4$; Fig. 17A) similarly to what observed in hippocampal networks ($\rho = 0.8$, $n = 5$; Fig. 17B and Bonifazi et al, 2005). The average latency increased with the physical distance between the recording electrode and the stimulating electrodes both in ES-derived and in hippocampal networks. The maximal speed of APs propagation was approximately 400mm/s both in ES-derived and in hippocampal networks (Fig. 17C and D and Bonifazi et al, 2005).

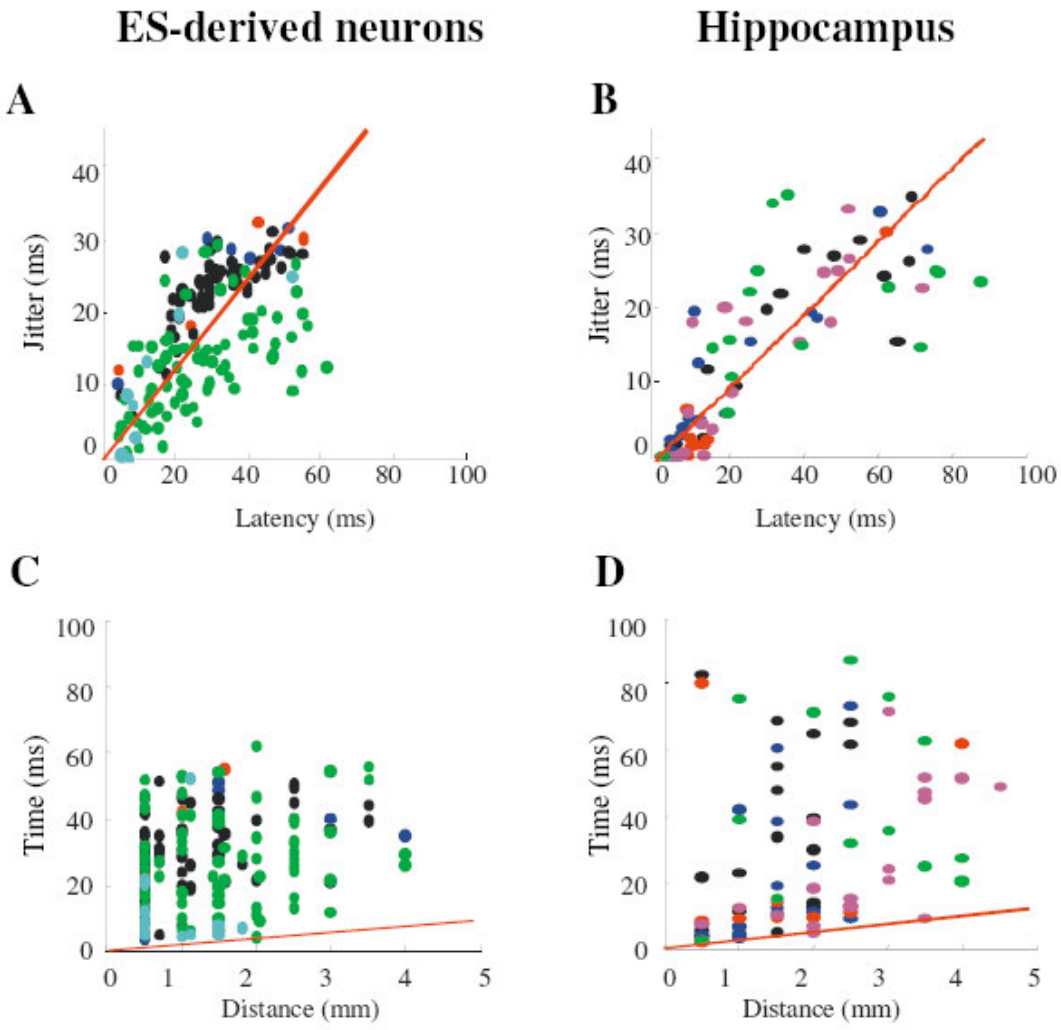

Figure 17. (A),(B): relation between jitter and latency of first evoked AP in ES-derived culture and hippocampal culture respectively. The line slope indicates the maximum speed of propagation of APs in the cultures approximately 400mm/s for both ES-derived neurons **(C)** and hippocampus **(D)**. Different colors represent different cultures.

The results shown in Figure 16 and 17 indicate that the evoked electrical activity in ES-derived networks spread with properties that are very similar to those observed in hippocampal networks.

3.7 REPRODUCIBILITY OF THE RESPONSE AND INFORMATION PROCESSING

Neurons under certain network conditions fire APs in a poorly reproducible way and in particular neurons receiving the same stimulation in different trials, fire a variable number of APs or the same number of APs but with a different timing (Arisi et al, 2001; Bonifazi et al, 2005; Zoccolan et al, 2002). In most trials the first evoked AP occurred with approximately the same latency and it is considered reliable (Bonifazi et al, 2005; Jimbo et al, 2000). Variability is characterized by repeatedly applying the same stimulation and analyzing the evoked average firing rate (AFR) and the corresponding coefficient of variation ($CV = \sigma_{AFR}/AFR$) defined as the ratio between the standard deviation of the AFR (σ_{AFR}) and the AFR itself. As shown in Figure 18A, for selected individual ES-derived neurons, the CV (black dots) of the AFR (white bars) was rarely lower than 0.5 indicating that the evoked electrical activity was not reproducible.

The variability of the evoked electrical activity can be significantly reduced when several neurons are considered and evoked APs are averaged or pooled together (Bonifazi et al, 2005; Johansson and Birznieks, 2004; Pinato et al, 2000; Zoccolan et al, 2002). When APs recorded from all the active electrodes (i.e. therefore from an ensemble of more than 30 ES-derived neurons) were pooled, the CV of the evoked activity was lower than 0.5 for 60 ms (Fig. 18B). A similar behavior was observed when the firing of individual hippocampal neurons were analyzed (Fig. 18C) and when their evoked electrical activity was pooled together, as shown in Figure 18D.

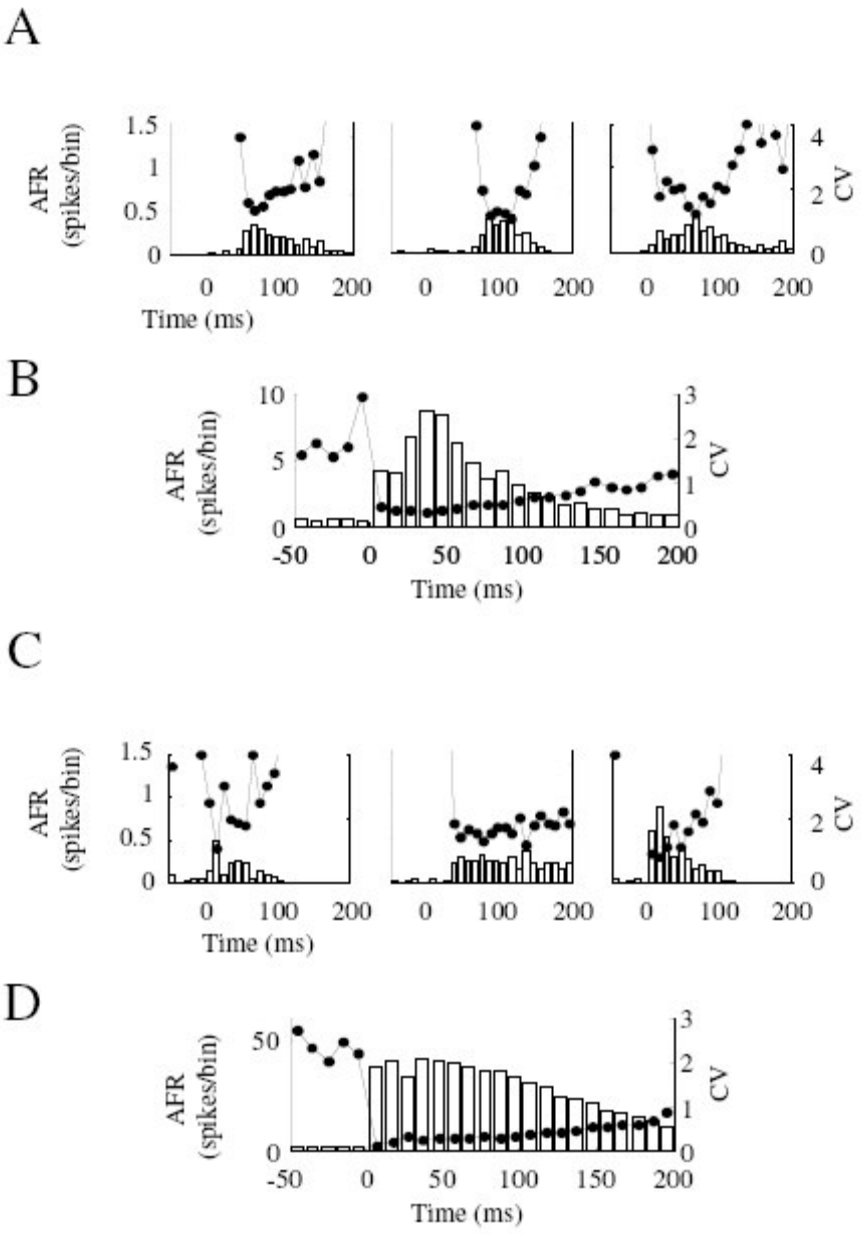

Figure 18. Reproducibility and coding. Average firing rate (AFR; open bars) and coefficient of variation (CV; black dots) of the firing from three selected embryonic stem cell (ES)-derived neurons **(A)** and from the entire network **(B)**. **(C)** and **(D)** as in **(A)** and **(B)**, but for neurons from hippocampal culture.

Functional neuronal networks, can process information by encoding important features of the stimulus such as its intensity (Bonifazi et al, 2005). Therefore, coding of stimulus intensity in ES-derived networks was investigated at the level of a single neuron

or when APs from a population of cells were pooled. The same analysis was carried out in hippocampal networks (Fig. 19).

Since pooling APs in ES-derived neurons exhibited a reproducible response (CV<0.5), we investigated whether ES-derived networks distinguish the stimulus intensity as observed in hippocampal networks (Bonifazi et al, 2005). Voltage pulses of different intensities were applied to the same row of electrodes. Raster plots of the evoked electrical activity from four distinct electrodes are shown in the four columns of Figure 19A. Similar data obtained from hippocampal networks are shown for comparison in Figure 19D. In both networks, by increasing the intensity of the voltage pulse from 300 to 600 and to 900 mV, the number of APs recorded on each electrode increased and the evoked APs became more frequent and more reliable.

When the evoked electrical activity among several dozens of ES-derived neurons was pooled, it was possible to reliably distinguish the three stimulus intensities. As shown in Figure 19B, the histograms of the evoked electrical activity from about three dozens of neurons for the three voltage stimuli were well separated. Therefore, ES-derived networks were able to distinguish the stimulus intensity as hippocampal networks do (Fig. 19E).

In order to quantify the ability of ES-derived networks to process information, we computed the mutual information IM, calculating the amount of information that could be decoded. As shown in Figure 19C, IM depended on the considered bin width and the size of neuronal pooling. With a bin width of 35 ms and by pooling the electrical activity from 20 electrodes about 1.3 bits of information were extracted from a theoretical maximum of 1.52 bits.

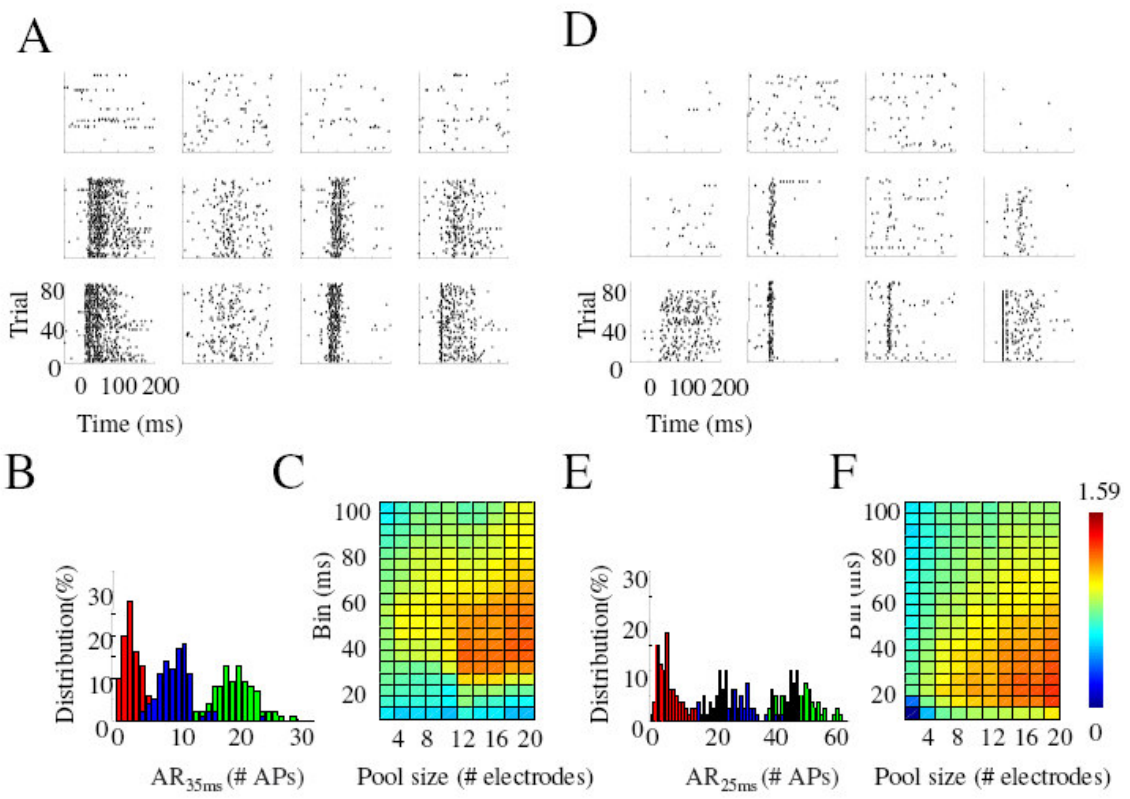

Figure 19. Information processing in embryonic stem cell (ES)-derived and hippocampal networks. **(A):** Raster plots of evoked action potentials (APs) recorded from four different electrodes (each column) by voltage pulses of 300, 600, and 900 mV (each row). **(B):** frequency histograms of all APs recorded in a time window from 0 to 51 ms from the stimulus evoked by the three different voltage stimulations. **(C):** Dependence of the mutual information on bin width and number of pooled electrodes. **(D, E, F):** As in **(A)**, **(B)**, and **(C)**, but from hippocampal cultures. In **(B)** and **(E)**, red corresponds to 300 mV, blue to 600 mV, and green to 900 mV.

Similar results were obtained in hippocampal networks where a maximum of 1.4 bits could be extracted by using a bin width of 25 ms and pooling the activity over 20 electrodes. These results show that ES-derived networks possess some basic computational properties as we previously demonstrated for hippocampal networks (Bonifazi et al, 2005).

3.8 NETWORK PROPERTIES WITH INTRACELLULAR RECORDINGS

The basis of network connectivity is the formation of functional synapses among different components. We therefore analyzed pharmacologically the different transmitters contribution to spontaneous postsynaptic events.

Starting from 14 days of differentiation, in most cultures intracellular recordings showed both excitatory and inhibitory spontaneous synaptic activity (Fig. 20). The identification of inhibitory synaptic contributions was performed by current clamp whole cell patch clamp recordings. In order to enhance the contribution of chloride currents, some experiments were performed in symmetrical chloride conditions where chloride mediated synaptic events result as depolarizing potentials. Addition of glutamate receptor blockers D-AP5 (30 μM) and CNQX (20 μM) allowed isolating inhibitory contributions. At resting potential the cells showed strong spontaneous depolarizing events that could trigger action potential initiation (Fig. 20, left trace). Further addition of the GABA-A antagonist SR-95531 (gabazine, 10 μM) completely canceled this spontaneous activity (Fig. 19A, right trace, n=3). These results demonstrate the contribution of GABAergic transmission in the spontaneous activity of ES-derived neurons. The averaged membrane potential before application of gabazine (Fig. 20A, left trace) calculated in a time window without occurrence of APs was -56 ± 5.4 mV, while after the application of gabazine, the averaged value in a time window of the same duration was -70 ± 1.1 mV. The decrease in the standard deviation reflected the block of chloride-mediated depolarization after gabazine treatment.

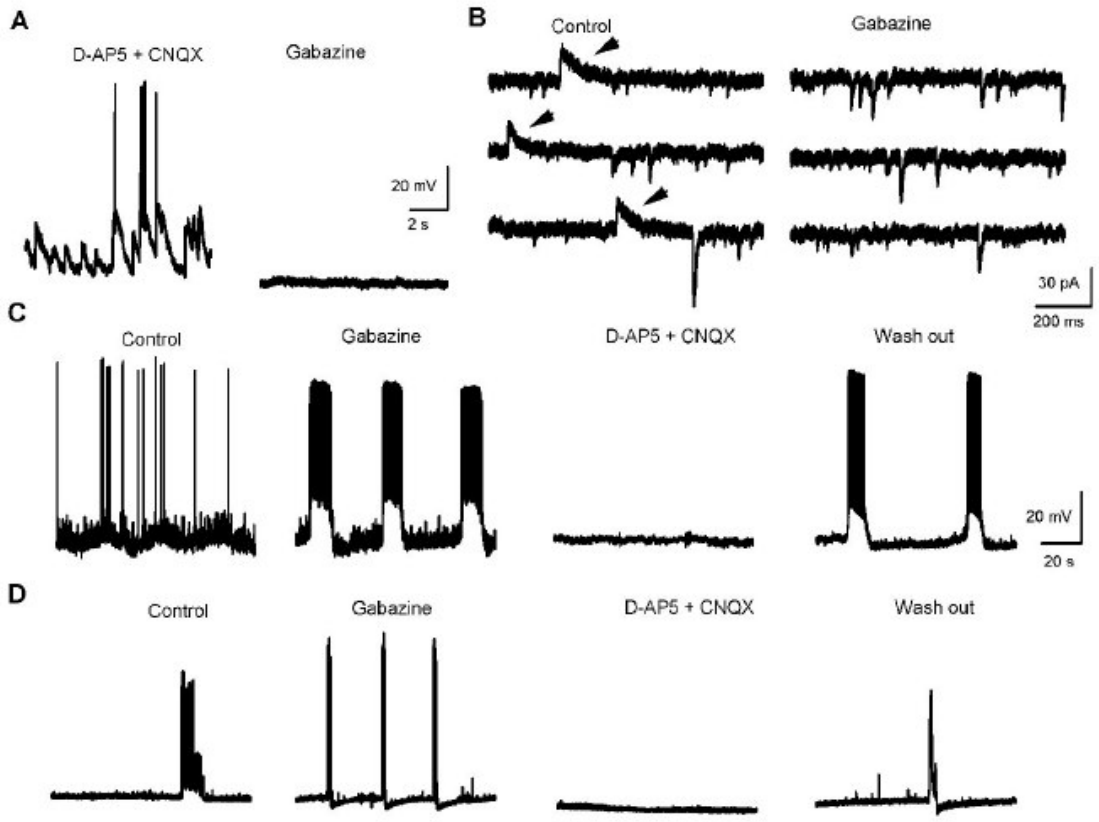

Figure 20. Electrophysiological and pharmacological identification of spontaneous synaptic inputs. **(A):** Whole-cell current-clamp patch-clamp recording at 0 bias current of an embryonic stem cell (ES)-derived neuron in presence of D-AP5 (30 μM) and CNQX (20 μM). The recording was performed in symmetrical chloride conditions in order to enhance the contribution of chloride currents (first trace). Addition of gabazine (10 μM) abolished the spontaneous activity, with a hyperpolarizing effect on the membrane potential (second trace). **(B):** Spontaneous outward (arrows) and inward currents were observed in voltage clamp recordings at −50 mV with potassium-gluconate-based pipette solution. Traces in left column are representative of control conditions, showing both outward and inward currents. Addition of gabazine completely prevented outward currents, but did not influence inward currents occurrence (representative traces in right column). **(C):** Spontaneous activity of ES-derived neuron recorded in current clamp at 0 bias with potassium-gluconate-based pipette solution (first trace). Application of gabazine synchronized excitatory synaptic inputs with consequent onset of bursts of action potentials (second trace). Further application of D-AP5 and CNQX completely abolished the occurrence of bursts (third trace). After wash out, bursting activity regenerated (last trace). **(D):** Hippocampal neuron spontaneous activity recorded in current clamp at 0 bias with potassium-gluconate-based pipette solution (first trace); effect of gabazine (second trace); effect of further addition of D-AP5 and CNQX (third) trace; and wash out (last trace). Traces scale as in C.

Further evidence for inhibitory contributions in the spontaneous synaptic activity could be found by recording the cells in voltage clamp conditions with K-gluconate based intracellular pipette solution (see methods) (Fig. 20B). By clamping the cell at -50 mV spontaneous occurring outward currents were recorded at a frequency of about 1Hz (see arrows in Fig. 20B). Subsequent application of gabazine completely prevented the occurrence of such events.

Excitatory synaptic input was also present in the spontaneous activity (Fig. 20C, control). Application of gabazine in K-gluconate based intracellular pipette solution to block inhibition both isolated excitatory contributions in whole cell patch clamp recordings and increased the synaptic coupling among the neurons participating to the network. This resulted in synchronous excitatory synaptic inputs in the recorded cells, often triggering bursts of APs (Fig. 20C, gabazine). In these conditions addition of glutamate receptor blockers D-AP5 and CNQX completely abolished the occurrence of such events (Fig. 20C, AP5; CNQX) that reappeared after wash out (Fig. 20C, wash out) (n=3).

The same experiment was also performed in hippocampal cells and data are shown in Fig. 20D (n=3). These results show the presence of inhibitory and excitatory synaptic contributions both for ES-derived and hippocampal neurons. However, difference in the firing pattern between the 2 networks was observed. In particular, the duration of the burst in the ES-derived neurons was significantly longer (13.4 ± 5.2s) than the hippocampal bursts (3.5 ± 1.3; *Student's t-test* $p<0.0005$).

3.9 WORK IN PROGRESS AND FUTURE PERSPECTIVES

The neuronal growth cone is the motile sensory structure at the end of the axon that detects extracellular guidance cues and integrates this information into directional movement towards the target cell. F-actin is the primary cytoskeletal element that maintains the growth cone shape and is essential for proper axon guidance, whereas microtubules are essential for giving the axon structure and serve an important function in axon elongation (Dent and Gertler, 2003).

While the role of guidance molecules (Dickson, 2002), underlying signaling and of both the F-actin and microtubule cytoskeletons are well established for growth cone movements (Dent and Gertler, 2003; Schaefer et al, 2002), relatively little is known about the three-dimensional structures and mechanical properties of these dynamic neuronal structures and how signaling pathways control the cytoskeleton (Grzywa et al, 2006).

Surface topology of the extracellular matrix (ECM) to which the cell adheres via integrins not only offers structural support but also activates transduction signals that have a fundamental role in cell survival, differentiation and overall tissue organization and function. It is well established that micrometer-size features on a culture surface can affect migration, adhesion and morphology (Norman and Desai, 2006). Since ECM has topographic detail down to the nanometer-scale (e.g., the 66nm repeat banding of collagen fibers), by mimicking the nanoscale topographic features presented to cells, biomaterials are used in tissue engineering to induce the same effects (Evans et al, 2006; Norman and Desai, 2006).

Atomic force microscopy (AFM) offers the possibility to examine the ultra-structure of biological samples from single proteins to cells at the nanometer (nm) scale. Shortly after AFM invention (Binnig et al, 1986), researchers started to use it to probe a variety of cell types, including neurons and glial cells, both alive and fixed. A small number of AFM studies investigated neurons focusing on the cell body, axon, and synaptic vesicle structure; however, only a limited attempt was made to study neuronal growth cones in detail (Grzywa et al, 2006).

We are interested in investigating the morphology of ES-derived growth cones and whether the extracellular surface can influence the growth cone formation and extension. Moreover, we want to investigate the influence on elongation and morphology of growth cone induced by addition of different combination of cytokines that are able to selectively enrich for different neuronal subtypes.

To study this we will combine atomic force microscopy with fluorescence labeling of cytoskeleton elements (actin, neuron-specific tubulin) on fixed neuronal precursors after differentiation induction.

When neuronal precursors start to differentiate, they form growth cones that can exhibit a wide variety of shapes and sizes. They explore their environment looking for other neurons to connect. The extension and formation of neurites is a fast process and in less than 24 hours they already reach other cells and make contacts with them. First of all, we tested different times of differentiation to select the sample that better suited the AFM analysis. We chose 12 hrs of differentiation because after 6 hours of differentiation induction neuronal precursors were weakly attached to the surface and they did not show the elongated shape, typical of neurons. On the other hand, after 24 or 48 hours of

differentiation, the cells had processes that were too long with few free growth cones, and they were difficult to examine. We started our observation by using the standard protocol described in this thesis without the use of specific neurotrophins.

Our preliminary results indicate that, while most of the ES-derived differentiating neurons show growth cones with a typical morphology (Fig. 21A), some "novel" structures were observed (Fig. 21B). These structures stain negatively for F-actin (Fig. 21C and D) and have halls that could be composed of residual cell membrane parts. We hypothesize that these structures are what is left during the retraction of the growth cones. In other words, before (or during) the retraction of growth cones, actin filaments are depolymerized while the cell membrane is, at least in part, lost.

Future experiments:

1) comparison of untreated glass coverslips with glass coverslips treated with reactive-ion etching (RIE) to obtain different degree of roughness,

2) comparison of shape and elongation rate of growth cones in the presence of different cytokines,

3) use of a gold surface with a nanophase surface roughness on micro-metric surface topology.

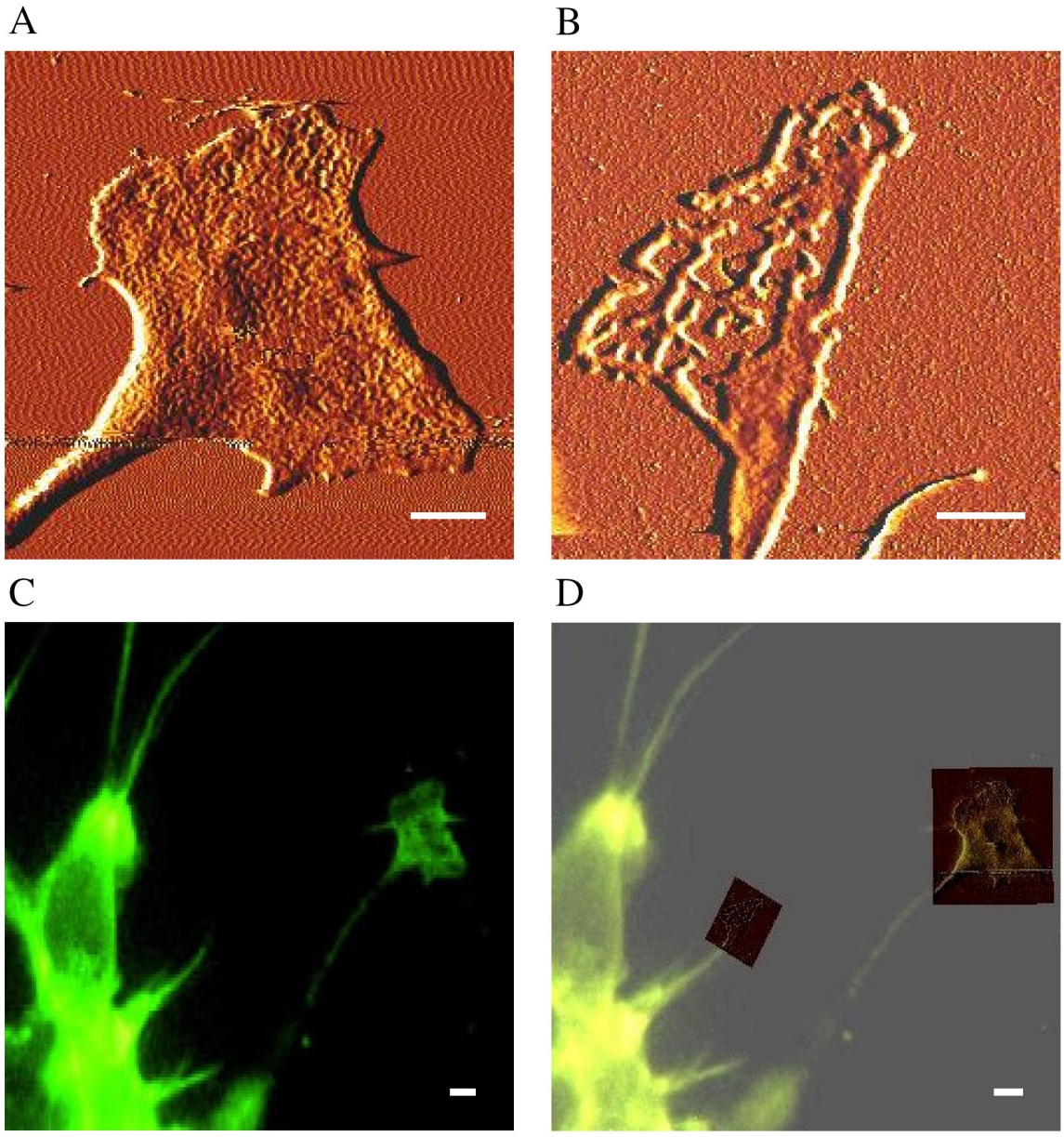

Figure 21. Atomic force microscope (AFM) image of growth cone with typical morphology **(A)** and "novel" structure **(B)** of ES-derived neurons at 12 hours of differentiation. **(C):** Immunofluorescence staining for F-actin and **(D):** the same as (C) but merged for the position of 2 structures showed in (A) and (B) analyzed by AFM. Scale bar = 2µm.

Before testing the different substrates with AFM we will perform a pre-screening of cell adhesion and growth by using a conventional immunofluorescence analysis. Preliminary tests by plating ES-derived neuronal precursors on glass or gold substrates

showed that for all glass samples the precoating with polyornithine and serum was required for adhesion and differentiation to occur, whereas on gold substrates neurons attached without any coating and seemed to differentiate even better than in standard culture conditions.

Understanding the influence of the substrate structure on both cell adhesion and differentiation will be of great interest, in particular for its future use in tissue engineering and regenerative medicine.

4. DISCUSSION

In the present work, we provide the first investigation to our knowledge of the formation of functional ES-derived neuronal networks and parallel processing of ES-derived networks.

4.1 ES CELLS AS SOURCE OF NEURONS AND PROTOCOLS FOR NEURONAL DIFFERENTIATION OF ES CELLS

We decided to use ES cells to obtain neurons and neuronal networks since they offer many advantages. First, ES cells represent virtually an unlimited source of cells compared to primary cell cultures where homogenous cell populations are difficult to obtain in sufficient quantities. The use of ES cells also reduces the number of animals that have to be sacrificed to obtain desired cell quantity.

Second, every ES-derived cell preparations derive from the same ES cell line thus avoiding the individual variability (from animal to animal) of the primary cell culture preparations.

Third, with *in vitro* protocol for neuronal differentiation, pluripotent ES cells pass from a totally uncommitted phenotype to one that strongly resembles mature neurons without ever having experienced a normal *in vivo* environment. Acquisition of the neuronal phenotype does not require exposure to the intact embryo, but can occur entirely *in vitro* (Finley et al, 1996) and can be controlled by modifying the external medium conditions (Barberi et al, 2003). Nonetheless, the wide range of powerful genetic

manipulations that are possible in ES cells allow a number of experiments to be performed that are difficult or impossible in primary cell cultures or in immortalized cell lines (Hancock et al, 2000).

Fourth, given the extensive efforts in this field over the past decade, several different protocols have evolved to promote neuronal differentiation of ES cells (Bibel et al, 2004; Lee et al, 2000; Li et al, 1998; Morizane et al, 2002; Okabe et al, 1996; Barberi et al, 2003; Westmoreland et al, 2001).

One of the earliest protocols employed the retinoic acid (RA) to induce neuronal differentiation, in the absence of any added cytokines or specific growth factors (Bain et al, 1995; Fraichard et al, 1995), and in agreement with some lines of researches that described neural induction as the derepression of a default state (Green, 1994). However, since RA is a strong teratogen and RA treatment of early embryos causes suppression of the forebrain development, it is supposed to perturb neuronal patterning and neuronal identities *in vitro* as it does *in vivo*. It is therefore preferable to avoid RA treatment for therapeutic applications or basic neuroscience research (Kawasaki et al, 2000).

Other researchers developed a selective method (also called V stages protocol) to obtain neurons and produce a good proportion of neuronal cells (Bibel et al, 2004; Hancock et al, 2000; Lee et al, 2000; Okabe et al, 1996; Westmoreland et al, 2001). The differentiation protocol involves several steps and one needs to select and amplify nestin-positive cells for a long time (14 days) before inducing differentiation (>24 days in total). In addition, EBs contain increased numbers of endodermal and mesodermal derivatives and this inherent heterogeneity makes identification and control of factors involved in specific NSC differentiation very difficult (Kawasaki et al, 2000; O'Shea, 1999).

The third approach involves the coculture of ES cells with stromal feeder cells that promote neuronal differentiation of ES cells without inducing mesodermal markers. This neuron-inducing effect was named stromal cell-derived inducing activity (SDIA) (Barberi et al, 2003; Kawasaki et al, 2000; Morizane et al, 2002). This method is fast, efficient and compared to earlier techniques, the induction of neuronal differentiation is more robust and exhibits minimal variability in obtaining neuronal cells (Barberi et al, 2003). This method also mimics the time course of early development (Kawasaki et al, 2000; Morizane et al, 2002).

The main advantage of this method is the possibility to selectively enrich neuronal culture with different neuronal subtypes (Barberi et al, 2003) and, mainly for this reason, we decided to use this protocol to obtain neurons.

Interestingly, the molecular nature of SDIA still remains to be identified. Two possibilities have been proposed (Kawasaki et al, 2000): one is that SDIA consists of two different neural-inducing factors, one that is anchored to the cell surface and one that is secreted. Another scenario is that secreted factors that are secondarily tethered to the cell surface are responsible for the activity (Morizane et al, 2006).

As a result of these findings, the determination of the molecular mechanism of SDIA will be indispensable because undefined factors produced by stromal cells may influence the differentiation of the ES cells to undesired cell types. An additional problem with this method is the difficulty that can be encountered when attempting to separate the ES-cell-derived cells from the stromal cells (Keller, 2005; Morizane et al, 2006).

The modification to the original protocol that we introduced (on day 6 of coculture and before the amplification step; see Methods) resulted in the efficient

separation of ES-derived cells from the stromal feeder after SDIA induction but before the network formation. The amplification of ES-derived neuronal precursors allowed us to induce their differentiation directly on the MEA and to establish good contact with the electrodes.

4.2 MATURATION AND SURVIVAL OF ES-DERIVED NEURONS AND CELLULAR HETEROGENEITY

Our data demonstrate that purely ES-derived neurons undergo functional maturation at a rate comparable to that observed after coculturing ES cells on top of a hippocampal slice (Benninger et al, 2003). The appearance of neuronal postmitotic markers occurred much earlier than the electrophysiological maturation of neurons.

The composition of our culture changed in terms of increased number of glial cells, slightly decreased number of neurons and the presence of non-neuronal cells during the observation period. An increase in glial cells reflected the prolonged period of *in vitro* differentiation required for network formation. Increased numbers of GFAP-positive cells over time is in agreement with *in vivo* developmental progression and with neural stem cell differentiation studies *in vitro* (Sauvageot and Stiles, 2002; Sun et al, 2003). This also indicated that a prolonged follow-up of the culture for therapeutic purposes is required.

The decrease in neuronal viability with time was also observed with RA protocol (Fraichard et al, 1995) while in many other cases it was not reported probably because the cells were analyzed during the first two or three weeks of differentiation (Bain et al,

1995; Barberi et al, 2003; Bibel et al, 2004; Hancock et al, 2000; Kawasaki et al, 2000; Nakayama et al, 2004; Okabe et al, 1996; Westmoreland et al, 2001; Ying et al, 2003).

We were able to culture ES-derived neurons and record extracellular signals on MEAs up to 10 weeks which is comparable to the viability of hippocampal culture. We found no available data of prolonged (>4weeks*) in vitro* survival of ES-derived neurons as we obtained with our cultures.

A major problem that remains to be solved in using ES cells to generate neurons is cellular heterogeneity within the cultures. None of the approaches used on murine ES cells has yet been shown to give 100% yield of cells with the required phenotype despite the use of growth factors and cytokines favoring differentiation of a particular neuronal cell type (Bibel et al, 2004; Evans et al, 2006; Keller, 2005; Lee et al, 2000; O'Shea, 1999).

Therefore, the presence of non-neuronal cells in our cultures (approximately 20% at three weeks of differentiation) was not surprising considering the wide differentiation potential of ES cells. In addition, the use of FCS at the beginning of differentiation (required for coating and inactivation of the trypsin), enhanced the formation and proliferation of non-neuronal cells.

Despite the fact that the use of FCS has several serious drawbacks including batch-to-batch variability and the lack of identity of the inducing factors contained in it (Keller, 2005), FCS is widely used at low concentrations (usually from 2-5%) in cultures of dissociated rat hippocampal and cortical cells (Benninger et al, 2003; Ruaro et al, 2005; Jimbo et al, 1999 and 2000).

To avoid the use of FCS in the differentiation step we tried to use the mechanical dissociation with HBSS solution (that does not require neutralization with FCS) before plating on MEA but this resulted in a decreased maturation of glial cells. Since glial cells secrete survival factors for the neurons, and also form an adhesive substratum for the neuronal cells *in vitro* (O'Shea, 1999), the decrease in glial formation affected negatively the adhesion and survival of neurons.

Since we could not avoid the use of FCS, to block non-neuronal cell proliferation, we tried to treat cells with Mitomycin C or Ara-C at different time points after the differentiation induction but this resulted in cell death and detachment from MEA plates. These observations suggest that ES-derived neurons are more sensitive than other cell types to proliferation blockers since the equal concentration of these agents conventionally used in primary cell cultures resulted toxic.

Recently we succeeded in treating the culture with Mitomycin C (at 10 days of differentiation when glial cells differentiate intensively) without causing enhanced neuronal cell death by lowering the incubation time and concentration used (the treatment consisted in 2 hours instead of overnight treatment at 1μg/ml of Mitomycin C which is 10-times less) but we now need to test the functional aspect of Mitomycin C-treated ES-derived neurons since morphological appearance is not predictive of electrophysiological properties.

To solve the problem of culture heterogeneity, methods to purify the populations and selection strategies are developing, especially if the cells are used for transplants (Evans et al, 2006; Ying et al, 2003). The neuronal precursors can be purified to homogeneity by fluorescence activated cell sorting (FACS) or drug selection (Ying et al,

2003). Alternatively, Jügling et al (2003) developed an immunoisolation procedure to purify neurons from *in vitro* differentiated mouse ES cells using an antibody against the neuronal cell adhesion molecule L1.

4.3 MEA AND NETWORK PROPERTIES OF ES-DERIVED NEURONS

The study of neuronal networks *in vitro* is conceivable because it has been shown that functional characteristics of *ex vivo* neuronal networks are similar to those observed *in vivo* in terms of connectivity, inhibition/excitation ratio, electrophysiological and electrical stimuli (for a review, see Van Pelt et al, 2004). Moreover, *in vitro* networks possess information-processing ability with basic computational properties similar to those found in *in vivo* networks (Fraichard et al, 1995). Recent work in our laboratory using dissociated hippocampal networks has also shown that different decoding strategies can be used to extract relevant features (Bonifazi et al, 2005), giving the appropriate parameters to investigate ES-derived networks. By culturing ES-derived neurons over a MEA, we show that these networks are functional and exert some computational properties similar to those of hippocampal networks in culture. When an extracellular voltage pulse was applied to the MEA electrodes, electrical activity was evoked and propagated for several millimeters in the culture with a velocity of approximately 400 mm/second, similar to that observed in hippocampal cultures. The firing pattern of neurons in response to the stimulus was mainly composed by a first, reliable AP followed by less reliable APs, again comparable to hippocampal (Bonifazi et al, 2005) and cortical

(Jimbo et al, 2000; Tateno et al, 2005) neuronal networks *in vitro*. The variability of firing in ES-derived neurons was reduced when the APs were pooled over a population of neurons, and the high reproducibility of the pooled response allowed distinguishing, at the level of a single trial, stimuli varying in intensity. The ability of ES-derived neurons to process information was illustrated by measuring the mutual information between the evoked response and the stimulus intensity. This analysis indicates that a population of ES-derived neurons can reliably discriminate three stimulus intensities (corresponding to 1.52 bits of information) as observed in naturally matured neurons (Bonifazi et al, 2005) and that ES-derived neurons can process information as mature neurons do. Despite the striking similarity observed in the evoked activity, we observed some differences in the spontaneous activity. Although bursts of synchronous firing were present in both networks, interburst activity was more prominent in the ES-derived networks (Fig. 14), reminiscent of immature hippocampal networks (data not shown). This could reflect a difference in the ongoing maturational process characterized by different numbers of gap junctions, differential voltage-gated channel and ligand receptor expression and/or composition, difference in the rectifying function of the chloride ions (Antonucci et al, 2001; Ben-Ari, 2002; Cherubini et al, 1991; Connors et al, 1983; Clayton et al, 1998; Smith et al, 1995), or percentage of glia in the cultures. One or more of these factors could also explain the difference in the duration of firing observed in the patch-clamp experiments between the two networks (Fig. 20C and D).

4.4 FUTURE PERSPECTIVES WITH ES-DERIVED NEURONAL NETWORKS

The finding that ES-derived neurons form functional networks *in vitro* leads the way to a variety of new perspectives for future applications. ES cells are a potent source for the generation of various neuronal cell types, and by changing the composition of the culture, it is possible to promote the differentiation in specific neuronal types (Barberi et al, 2003; Morizane et al, 2002; Lee et al, 2000; Westmoreland et al, 2001). Therefore, in the near future, it will be feasible to engineer neuronal networks with different neuronal types and to investigate the properties of the resulting networks. Similarly, because ES cells are amenable to genetic modification (Friedrich and Soriano, 1991; Ying et al, 2003; Thomas and Capecchi, 1987), it will be possible to obtain neuronal types with modified properties in which selected ion channels or synaptic receptors are over- or underexpressed. This technology will allow the construction of neuronal networks with entirely new computational properties. The same technology can provide valid models of neuronal networks linked to a variety of neurodegenerative diseases and can verify the action of new ES-derived neurons on these model networks, providing a new perspective for therapeutic recovery.

The availability of unlimited number of ES-derived neurons paired with an intrinsic ability of these cells to form neuronal networks suggests the potential of this system to establishing large-scale, self-assembling networks. Such complex networks could provide a first key step towards ES cell-based neurocomputing (Bonifazi et al, 2005; Ruaro et al, 2005).

5. REFERENCES

Alison MR, Poulsom R, Forbes S, Wright NA. An introduction to stem cells. J Pathol. 2002 Jul; 197(4):419-23.

Antonucci DE, Lim ST, Vassanelli S, Trimmer JS. Dynamic localization and clustering of dendritic Kv2.1 voltage-dependent potassium channels in developing hippocampal neurons. Neuroscience. 2001; 108(1):69-81.

Arisi I, Zoccolan D, Torre V. Distributed motor pattern underlying whole-body shortening in the medicinal leech. J Neurophysiol. 2001; 86(5):2475-88.

Armstrong L, Saretzki G, Peters H, Wappler I, Evans J, Hole N, von Zglinicki T, Lako M. Overexpression of telomerase confers growth advantage, stress resistance, and enhanced differentiation of ESCs toward the hematopoietic lineage. Stem Cells. 2005 Apr; 23(4):516-29.

Baizabal JM, Furlan-Magaril M, Santa-Olalla J, Covarrubias L. Neural stem cells in development and regenerative medicine. Arch Med Res. 2003 Nov-Dec; 34(6):572-88.

Bain G, Kitchens D, Yao M, Huettner JE, Gottlieb DI. Embryonic stem cells express neuronal properties in vitro. Dev Biol. 1995 Apr; 168(2):342-57.

Barberi T, Bradbury M, Dincer Z, Panagiotakos G, Socci ND, Studer L. Derivation of engraftable skeletal myoblasts from human embryonic stem cells. Nat Med. 2007 May; 13(5):642-648.

Barberi T, Klivenyi P, Calingasan NY, Lee H, Kawamata H, Loonam K, Perrier AL, Bruses J, Rubio ME, Topf N, Tabar V, Harrison NL, Beal MF, Moore MA, Studer L. Neural subtype specification of fertilization and nuclear transfer embryonic stem cells and application in parkinsonian mice.Nat Biotechnol. 2003 Oct; 21(10):1200-7.

Ben-Ari Y. Excitatory actions of gaba during development: the nature of the nurture. Nat Rev Neurosci. 2002 Sep; 3(9):728-39.

Benninger F, Beck H, Wernig M, Tucker KL, Brustle O, Scheffler B. Functional Integration of Embryonic Stem Cell-Derived Neurons in Hippocampal Slice Cultures. J Neurosci. 2003 Aug 6; 23(18):7075-83.

Bibel M, Richter J, Schrenk K, Tucker KL, Staiger V, Korte M, Goetz M, Barde YA. Differentiation of mouse embryonic stem cells into a defined neuronal lineage. Nat Neurosci. 2004 Sep; 7(9):1003-9.

Binnig G, Quate CF, Gerber C. Atomic force microscope. Phys Rev Lett. 1986 Mar 3; 56(9):930-3.

Bishop AE, Buttery LD, Polak JM. Embryonic stem cells. J Pathol. 2002 Jul; 197(4):424-9.

Bonifazi P, Ruaro ME, Torre V. Statistical properties of information processing in neuronal networks. Eur J Neurosci. 2005 Dec; 22(11):2953-64.

Brüstle O, Jones KN, Learish RD, Karram K, Choudhary K, Wiestler OD, Duncan ID, McKay RD. Embryonic stem cell-derived glial precursors: a source of myelinating transplants. Science. 1999 Jul 30; 285(5428):754-6.

Canepari M, Bove M, Maeda E, Cappello M, Kawana A. Experimental analysis of neuronal dynamics in cultured cortical networks and transition between different patterns of activity. Biol Cybern 1997 Aug; 77(2):153-62.

Cherubini E, Gaiarsa JL, Ben-Ari Y. GABA: an excitatory transmitter in early postnatal life. Trends Neurosci. 1991 Dec; 14(12):515-9.

Clayton GH, Staley KJ, Wilcox CL, Owens GC, Smith RL. Developmental expression of C1C-2 in the rat nervous. system. Brain Res Dev Brain Res. 1998 Aug; 108(1-2):307-18.

Connors BW, Bernardo LS, Prince DA. Coupling between neurons of the developing neocortex. J. Neurosci. 1983 Apr; 3(4):773-82.

Corner MA. Reproducibility of structure-function relations in developing neuronal networks- the odyssey of self-organizing brain through research fads, fallacies and prospects. Prog. Brain Res. 1994; 102:3-31.

Dayan P, Abbott LF. Theoretical Neuroscience. Computational and mathematical modeling of neural systems. MIT Press. Cambridge, Massachusets, 2001.

DeCharms RC, Merzenich MM. Primary cortical representation of sounds by the coordination of action-potential timing. Nature. 1996; 381:610-3.

Demas J, Eglen SJ, Wong RO. Developmental loss of synchronous spontaneous activity in the mouse retina is independent of visual experience. J Neurosci. 2003; 23:2851-60.

Dickson BJ. Molecular mechanisms of axon guidance. Science. 2002 Dec 6;298(5600):1959-64. Review. Erratum in: Science. 2003 Jan 24; 299(5606):515.

Dent EW, Gertler FB. Cytoskeletal dynamics and transport in growth cone motility and axon guidance. Neuron. 2003 Oct 9; 40(2):209-27.

Evans MJ, Kaufman MH. Establishment in culture of pluripotential cells from mouse embryos. Nature. 1981 Jul 9; 292(5819):154-6.

Egert U, Knott T, Schwarz C, Nawrot M, Brandt A, Rotter S, Diesmann M. MEA-Tools: an open source toolbox for the analysis of multi-electrode data with MATLAB. J Neurosci Meth. 2002; 17:33-42.

Evans ND, Gentleman E, Polak JM. Scaffolds for stem cells. Materialstoday. 2006 Dec; 9(12):26-33.

Finley MF, Kulkarni N, Huettner JE. Synapse formation and establishment of neuronal polarity by P19 embryonic carcinoma cells and embryonic stem cells. J Neurosci. 1996 Feb 1; 16(3):1056-65.

Fraichard A, Chassande O, Bilbaut G, Dehay C, Savatier P, Samarut J. In vitro differentiation of embryonic stem cells into glial cells and functional neurons. J Cell Sci. 1995 Oct; 108 (Pt 10):3181-8.

Friedrich G, Soriano P. Promoter traps in embryonic stem cells: a genetic screen to identify and mutate developmental genes in mice. Genes Dev 1991; 5:1513-23.

Georgopoulos AP, Schwartz AB, Kettner RE. Neuronal population coding of movement direction. Science. 1986; 233:1416-9.

Gottlieb DI. Large-scale sources of neural stem cells. Annu Rev Neurosci. 2002; 25:381-407.

Gray CM, Konig P, Engel AK. Singer W. Oscillatory responses in cat visual cortex exhibit inter-columnar synchronization which reflects global stimulus properties. Nature. 1989; 338(6213):334-7.

Green JB. Roads to neuralness: embryonic neural induction as derepression of a default state. Cell. 1994 May 6; 77(3):317-20.

Grzywa EL, Lee AC, Lee GU, Suter DM. High-resolution analysis of neuronal growth cone morphology by comparative atomic force and optical microscopy. J Neurobiol. 2006 Dec; 66(14):1529-43.

Hancock CR, Wetherington JP, Lambert NA, Condie BG. Neuronal differentiation of cryopreserved neural progenitor cells derived from mouse embryonic stem cells. Biochem Biophys Res Commun. 2000; 271:418-21.

Hara A, Niwa M, Kunisada T et al. Embryonic stem cells are capable of generating a neuronal network in the adult mouse retina. Brain Res. 2004; 999:216-21.

Hopfield JJ. Neural networks and physical systems with emergent collective computational ability. Proc Nat Acad Sci U S A 1982; 79:2554-58.

Hopfield JJ. Pattern recognition computation using action potential timing for stimulus representation. Nature. 1995; 376:33-6.

Huettner JE, Baughman RW. Primary culture of identified neurons from the visual cortex of postnatal rats. J Neurosci. 1986; 6:3044-60.

Jiang YQ, Oblinger MM. Differential regulation of beta III and other tubulin genes during peripheral and central neuron development. J Cell Sci. 1992 Nov; 103 (Pt 3):643-51.

Jimbo Y, Kawana A. Electrical stimulation and recording from cultured neurons using a planar microelectrode array. Bioelectrochem Bioenerg.1992; 29:193-204.

Jimbo Y, Kawana A, Parodi P, Torre V. The dynamics of a neuronal culture of dissociated cortical neurons of neonatal rats. Biol Cybern. 2000; 83(1):1-20.

Jimbo Y, Tateno T, Robinson H Simultaneous induction of pathway-specific potentiation and depression in networks of cortical neurons. Biophys J. 1999; 76:670-78.

Johansson RS, Birznieks I. First spikes in ensembles of human tactile afferents code complex spatial fingertip events. Nat Neurosci. 2004; 7:170-7.

Jüngling K, Nägler K, Pfrieger FW, Gottmann K. Purification of embryonic stem cell-derived neurons by immunoisolation. FASEB J. 2003; 7:2100-2.

Kamioka H, Maeda E, Jimbo Y, Robinson HP, Kawana A. Spontaneous periodic synchronized bursting during formation of mature patterns of connections in cortical cultures. Neurosci Lett. 1996; 206(2-3):109-12.

Kaufman MH, Robertson EJ, Handyside AH, Evans MJ. Establishment of pluripotential cell lines from haploid mouse embryos. J Embryol Exp Morphol. 1983 Feb; 73:249-61.

Kawasaki H, Mizuseki K, Nishikawa S, Kaneko S, Kuwana Y, Nakanishi S, Nishikawa SI, Sasai Y. Induction of midbrain dopaminergic neurons from ES cells by stromal cell-derived inducing activity. Neuron. 2000 Oct; 28(1):31-40.

Kennea NL, Mehmet H. Neural stem cells. J Pathol. 2002 Jul; 197(4):536-50.

Keller GM. In vitro differentiation of embryonic stem cells. Curr Opin Cell Biol. 1995 Dec; 7(6):862-9.

Keller G. Embryonic stem cell differentiation: emergence of a new era in biology and medicine. Genes Dev. 2005 May 15; 19(10):1129-55.

Kerr JND, Greenberg D, Helmchen F. Imaging input and output of neocortical networks in vivo. Proc Natl Acad Sci USA. 2005; 102:14063-8.

Kim JH, Auerbach JM, Rodriguez-Gomez JA, Velasco I, Gavin D, Lumelsky N, Lee SH, Nguyen J, Sanchez-Pernaute R, Bankiewicz K, McKay R. Dopamine neurons derived from embryonic stem cells function in an animal model of Parkinson's disease. Nature. 2002 Jul 4; 418(6893):50-6.

Lahtinen H, Palva JM, Sumanen S, Voipio J, Kaila K, Taira T. Postnatal development of rat hippocampal gamma rhythm in vivo. J Neurophysiol. 2002; 88(3):1469-74.

Lee H, Al Shamy G, Elkabetz Y, Schoefield CM, Harrsion NL, Panagiotakos G, Socci ND, Tabar V, Studer L. Directed Differentiation And Transplantation of Human Embryonic Stem Cell Derived Motoneurons. Stem Cells. 2007 May 3.

Lee SH, Lumelsky N, Studer L, Auerbach JM, McKay RD. Efficient generation of midbrain and hindbrain neurons from mouse embryonic stem cells. Nat Biotechnol. 2000 Jun; 18(6):675-9.

Lestienne R. Spike timing, synchronization and information processing on the sensory side of the central nervous system. Prog Neurobiol. 2001; 65:545-91.

Leinekugel X, Khazipov R, Cannon R, Hirase H, Ben-Ari Y, Buzsaki G. Correlated bursts of activity in the neonatal hippocampus in vivo. Science. 2002; 296(5575):2049-52.

Li M, Pevny L, Lovell-Badge R, Smith A. Generation of purified neural precursors from embryonic stem cells by lineage selection. Curr Biol. 1998 Aug 27; 8(17):971-4.

Limpert E, Stahel W.A, Abbot M. Log-normal distributions across the sciences: keys and clues. Bioscience 2001; 51:341-352.

Maeda E, Kuroda Y, Robinson HP et al. Modification of parallel activity elicited by propagating bursts in developing networks of rat cortical neurones. Eur J Neurosci. 1998; 10:488-96.

Maeda E, Robinson HP, Kawana A. The mechanisms of generation and propagation of synchronized bursting in developing networks of cortical neurons. J Neurosci. 1995; 15:6834-45.

Marom S, Shahaf G. Development, learning and memory in large random networks of cortical neurons: lessons beyond anatomy. Q Rev Biophys. 2002; 35:63-87.

Martin GR. Isolation of a pluripotent cell line from early mouse embryos cultured in medium conditioned by teratocarcinoma stem cells. Proc Natl Acad Sci U S A. 1981 Dec; 78(12):7634-8.

McDonald JW, Liu XZ, Qu Y, Liu S, Mickey SK, Turetsky D, Gottlieb DI, Choi DW. Transplanted embryonic stem cells survive, differentiate and promote recovery in injured rat spinal cord. Nat Med. 1999; 5:1410-2.

Miles GB, Yohn DC, Wichterle H, Jessel TM, Rafuse VF, Brownstone RM. Functional properties of motoneurons derived from mouse embryonic stem cells. J Neurosci. 2004; 24:7848-58.

Morin FO, Takamura Y, Tamiya E. Investigating neuronal activity with planar microelectrode arrays: achievements and new perspectives. J Biosci Bioeng. 2005 Aug; 100(2):131-43.

Morizane A, Takahashi J, Shinoyama M, Ideguchi M, Takagi Y, Fukuda H, Koyanagi M, Sasai Y, Hashimoto N. Generation of graftable dopaminergic neuron progenitors from mouse ES cells by a combination of coculture and neurosphere methods. J Neurosci Res. 2006 May 1; 83(6):1015-27.

Morizane A, Takahashi J, Takagi Y, Sasai Y, Hashimoto N. Optimal conditions for in vivo induction of dopaminergic neurons from embryonic stem cells through stromal cell-derived inducing activity. J Neurosci Res. 2002 Sep 15; 69(6):934-9.

Nakanishi K, Kukita F. Intracellular [Cl(-)] modulates synchronous electrical activity in rat neocortical neurons in culture by way of GABAergic inputs. Brain Res. 2000; 863:192-204.

Nakayama T, Momoki-Soga T, Yamaguchi K, Inoue N. Efficient production of neural stem cells and neurons from embryonic stem cells. Neuroreport. 2004; 15(3):487-91.

Neale EA, Oertel WH, Bowers LM, Weise VK. Glutamate decarboxylase immunoreactivity and gamma-[3H] aminobutyric acid accumulation within the same neurons in dissociated cell cultures of cerebral cortex. J Neurosci. 1983; 3(2):376-82.

Nicolelis MA, Ghazanfar AA, Faggin BM, Votaw S, Oliveira LM. Reconstructing the engram: simultaneous, multisite, many single neuron recordings. Neuron. 1997; 18(4):529-37.

Nicolelis MA, Ghazanfar AA, Stambaugh CR, Oliveira LM, Laubach M, Chapin JK, Nelson RJ, Kaas JH. Simultaneous encoding of tactile information by three primate cortical areas. Nat Neurosci. 1998; 1:621-30.

Norman JJ, Desai TA. Methods for fabrication of nanoscale topography for tissue engineering scaffolds. Ann Biomed Eng. 2006 Jan; 34(1):89-101.

Okabe S, Forsberg-Nilsson K, Spiro AC, Segal M, McKay RD. Development of neuronal precursor cells and functional postmitotic neurons from embryonic stem cells in vitro. Mech Dev. 1996 Sep; 59(1):89-102.

Okano H. Stem cell biology of the central nervous system. J Neurosci Res. 2002 Sep 15; 69(6):698-707.

O'Keefe J, Recce M. LPhase relationship between hippocampal place units and the EEG theta rhythm. Hippocampus 1993; 3:317-30.

O'Shea KS. Embryonic stem cell models of development. Anat Rec. 1999 Feb 15; 257(1):32-41.

Panzeri S, Treves A. Analytical estimates of limited sampling biases in different information measures. Network.1996; 7:87-107.

Perrier AL, Studer L. Making and repairing the mammalian brain - in vitro production of dopaminergic neurons. Semin Cell Dev Biol. 2003 Jun; 14(3):181-9.

Pinato G, Battiston S, Torre V. Statistical independence and neural computation in the leech ganglion. Biol Cybern. 2000; 83:119-30.

Potter SM. Distributed processing in cultured neuronal networks. Prog Brain Res. 2000; 130: 49-62.

Robinson HP, Kawahara M, Jimbo Y, Torimitsu K, Kuroda Y, Kawana A. Periodic synchronized bursting and intracellular calcium transients elicited by low magnesium in cultured cortical neurons. J Neurophysiol. 1993a; 70(4):1606-16.

Robinson HP, Torimitsu K, Jimbo Y, Kuroda Y, Kawana A. Periodic bursting of cultured cortical neurons in low magnesium - cellular and network mechanisms. *Jpn. J. Physiol.* 1993b; (Suppl. 43): l25-30.

Ruaro ME, Bonifazi P, Torre V. Toward the neurocomputer: image processing and pattern recognition with neuronal cultures. IEEE Trans Biomed Eng. 2005 Mar; 52(3):371-83.

Rumelhart DE, McClelland JL. Explorations in Parallel Distributed Processing. MIT Press. Cambridge, Massachusetts, 1998.

Rüschenschmidt C, Koch PG, Brüstle O, Beck H. Functional properties of ES cell-derived neurons engrafted into the hippocampus of adult normal and chronically epileptic rats. *Epilepsia* 2005; 46 (Suppl 5):174-8.

Sauvageot CM, Stiles CD. Molecular mechanisms controlling cortical gliogenesis. Curr Opin Neurobiol. 2002 Jun; 12(3):244-9.

Schaefer AW, Kabir N, Forscher P. Filopodia and actin arcs guide the assembly and transport of two populations of microtubules with unique dynamic parameters in neuronal growth cones. J Cell Biol. 2002 Jul 8; 158(1):139-52.

Shahaf G, Marom S. Learning in networks of cortical neurons. J Neurosci. 2001; 21:8782-8.

Shannon CE, Weaver W. The mathematical theory of communication. Urbana: University of Illinois Press, 1949.

Singer W, Gray C.M. Visual feature integration and the temporal correlation hypothesis. Ann Rev Neurosci. 1995; 18:555-86.

Smith RL, Clayton GH, Wilcox CL, Escudero KW, Staley KJ. Differential expression of an inwardly rectifying chloride conductance in rat brain neurons: a potential mechanism for cell-specific modulation of postsynaptic inhibition. J Neurosci. 1995; 15:4057-67.

Stosiek C, Garaschuk O, Holthoff K, Konnerth A. In vivo two-photon calcium imaging of neuronal networks. Proc Natl Acad Sci U S A. 2003 June 10; 100(12): 7319-24.

Strübing C, Ahnert-Hilger G, Shan J, Wiedenmann B, Hescheler J, Wobus AM. Differentiation of pluripotent embryonic stem cells into neuronal lineage in vitro gives rise to mature inhibitory and excitatory neurons. Mech Dev. 1995; 53:275-87.

Sun YE, Martinowich K, Ge W. Making and repairing the mammalian brain--signaling toward neurogenesis and gliogenesis. Semin Cell Dev Biol. 2003 Jun;14(3):161-8.

Tateno T, Jimbo Y, Robinson HP. Spatio-temporal cholinergic modulation in cultured networks of rat cortical neurons: spontaneous activity. Neuroscience. 2005;134:425-37.

Tateno T, Kawana A, Jimbo Y. Analytical characterization of spontaneous firing in networks of developing rat cultured cortical neurons. Phys Rev E Stat Nonlin Soft Matter Phys Phys. 2002; 65 (5 Pt 1) 051924.

Thomas KR, Capecchi MR. Site-directed mutagenesis by gene targeting in mouse embryo-derived stem cells. Cell 1987; 51:503-12.

Thomson JA, Itskovitz-Eldor J, Shapiro SS, Waknitz MA, Swiergiel JJ, Marshall VS, Jones JM. Embryonic stem cell lines derived from human blastocysts. Science. 1998 Nov 6;282(5391):1145-7. Erratum in: Science 1998 Dec 4;282(5395):1827.

Thomson JA, Kalishman J, Golos TG, Durning M, Harris CP, Becker RA, Hearn JP. Isolation of a primate embryonic stem cell line. Proc Natl Acad Sci U S A. 1995 Aug 15;92(17):7844-8.

Thorpe S, Delorme A, Van Rullen R. Spike-based strategies for rapid processing. Neural Network. 2001; 14:715-25.

Tsumura A, Hayakawa T, Kumaki Y, Takebayashi S, Sakaue M, Matsuoka C, Shimotohno K, Ishikawa F, Li E, Ueda HR, Nakayama J, Okano M. Maintenance of self-renewal ability of mouse embryonic stem cells in the absence of DNA methyltransferases Dnmt1, Dnmt3a and Dnmt3b. Genes Cells. 2006 Jul;11(7):805-14.

Van Pelt J, Vajda I, Wolters PS, Corner MA, Ramakers GJ. Dynamics and plasticity in developing neuronal networks in vitro. Prog Brain Res. 2005; 147:173-88.

Van Pelt J, Wolters PS, Corner MA, Rutten WL, Ramakers GJ. Long-term characterization of firing dynamics of spontaneous burst in cultured neural networks. IEEE Trans Biomed Eng. 2004; 51(11):2051-62.

Wagenaar DA, Pine J, Potter SM. Effective parameters for stimulation of dissociated cultures using multi-electrode arrays. J Neurosci Methods. 2004; 138:27-37.

Wagenaar DA, Potter SM. Real-time multi-channel stimulus artifact suppression by local curve fitting. J Neurosci Methods. 2002; 120:113-120.

Welsh DK, Logothetis DE, Meister M, Reppert SM. Individual neurons dissociated from rat suprachiasmatic nucleus express independently phased circadian firing rhythm. Neuron 1995.14; 697-706.

Wernig M, Benninger F, Schmandt T, Rade M, Tucker KL, Bussow H, Beck H, Brustle O. Functional Integration of Embryonic Stem Cell-Derived Neurons In Vivo. J Neurosci. 2004; 24:5258-68.

Westmoreland JJ, Hancock CR, Condie BG. Neuronal development of embryonic stem cells: a model of GABAergic neuron differentiation. Biochem Biophys Res Commun. 2001 Jun 15;284(3):674-80.

Ying QL, Stavridis M, Griffiths D et al. Conversion of embryonic stem cells into neuroectodermal precursors in adherent monoculture. Nat Biotechnol. 2003; 21:183-86.

Zoccolan D, Pinato G, Torre V. Highly variable spike trains underlie reproducible sensorimotor responses in the medicinal leech. J Neurosci. 2002; 22:10790-800.

Acknowledgments

First of all, I would like to thank my supervisor, Vincent Torre. I really appreciated working in his lab for the past five years. I admire his ability in putting together such a great group of people to work with, for his comprehension and encouragement during all this time.

I thank Dr. Lorenz Studer for giving us the ES and stromal cells.

I thank Ino and Fred for their work on network analysis, Giulietta for the patch-clamp experiments but most of all for their friendship. I thank Giada for preparing the hippocampal cultures and for taking care of our tissue culture room; Tullio, Gabriella, Massimo and Beatrice for technical assistance and in particular Francesco and Micaela for helping me with the confocal microscopy.

I thank Manuela for carefully reading my thesis, Amanda for her patience, Sergio and Libero for pc assistance.

I thank my group: Alby (I'm still your fan n.1!), SUPER-Silvia, Walter, Anil, Jummi, Rajesh, Pano, Daniela, Giacomo, Jacobo, Marco, Diana……. and my soul and desk mate, Monica.

I thank my dear and special friends Elizabeth and Andrea…

……and all SISSA people for being so nice to me, in particular Claudio and Cristina, Laura, Dejan, EA, Miranda, Paola, Matteo and Silvia, Marcelo, Helena……

Finally, the person that I owe so much to and that I sincerely thank is Elisabetta, for her patience, understanding, support, advices, teaching, encouragements, efforts, care…….THANK YOU SO MUCH!!!!!!!!!!!!!!

I'm grateful to my family, my husband and my little daughter Sara for their love and support.

J.B.